Passive Radar at ZESS – From HITCHHIKER to ASTRA

Otmar Loffeld, Holger Nies, Florian Behner, Simon Reuter
University of Siegen, Center for Sensor Systems

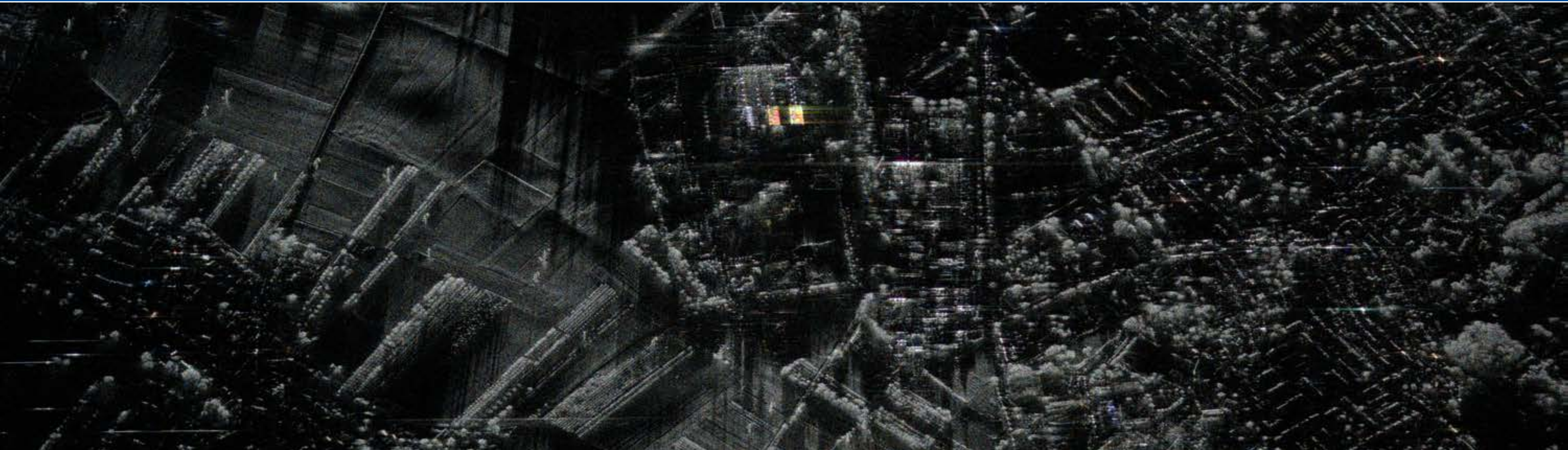

Overview of the project

HITCHHIKER

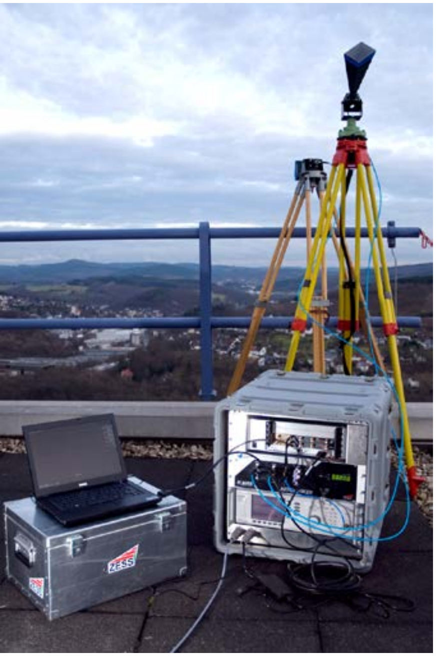

Overview of the project

HITCHHIKER

First Spaceborne-Stationary
Experiment with TerraSAR-X

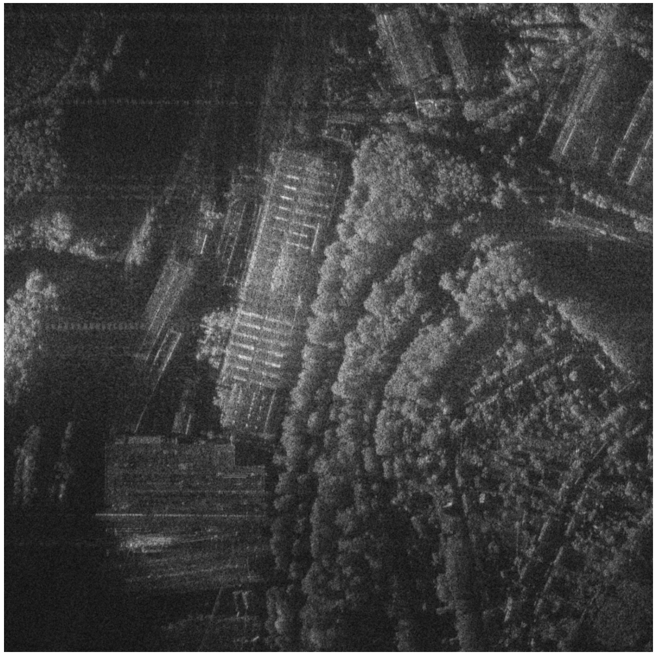

Overview of the project

HITCHHIKER

First Spaceborne-Stationary Experiment with TerraSAR-X

Repeat-Pass Interferometry Experiment

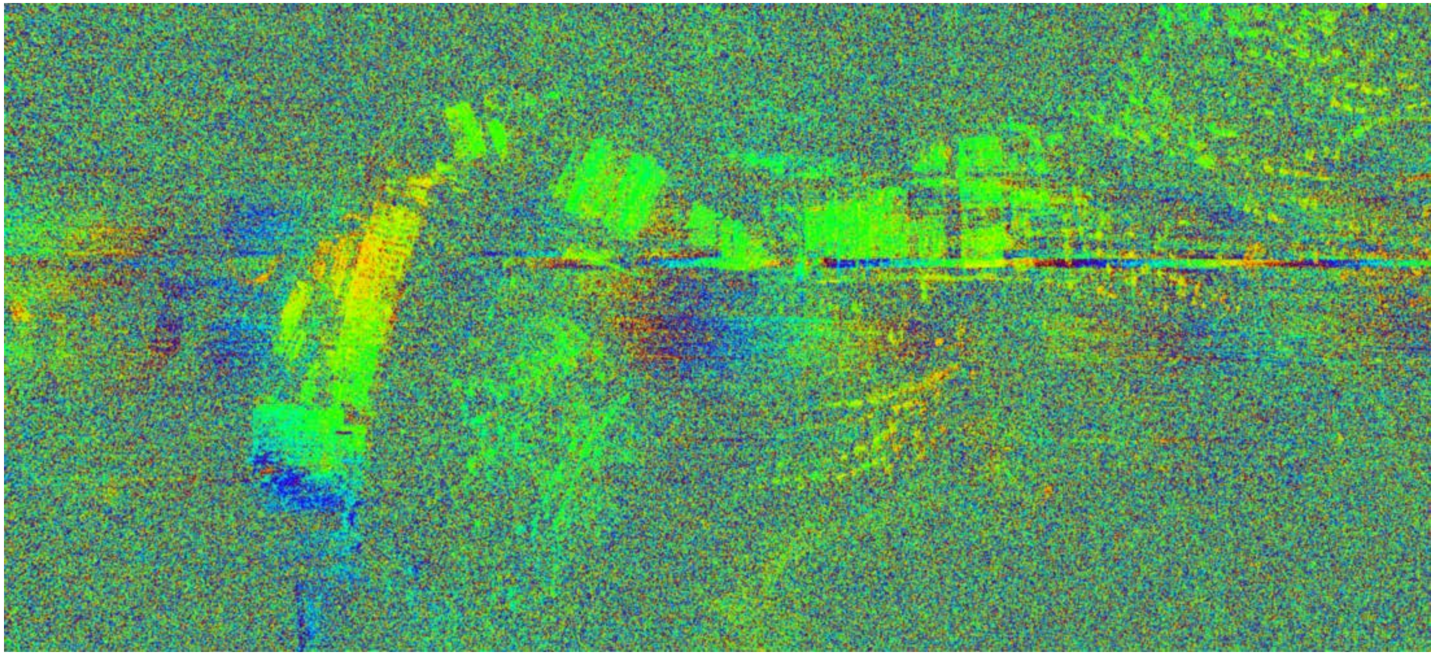

HITCHHIKER
4 Channel Extension

HITCHHIKER
4 Channel Extension

Single Pass Interferometry Experiment

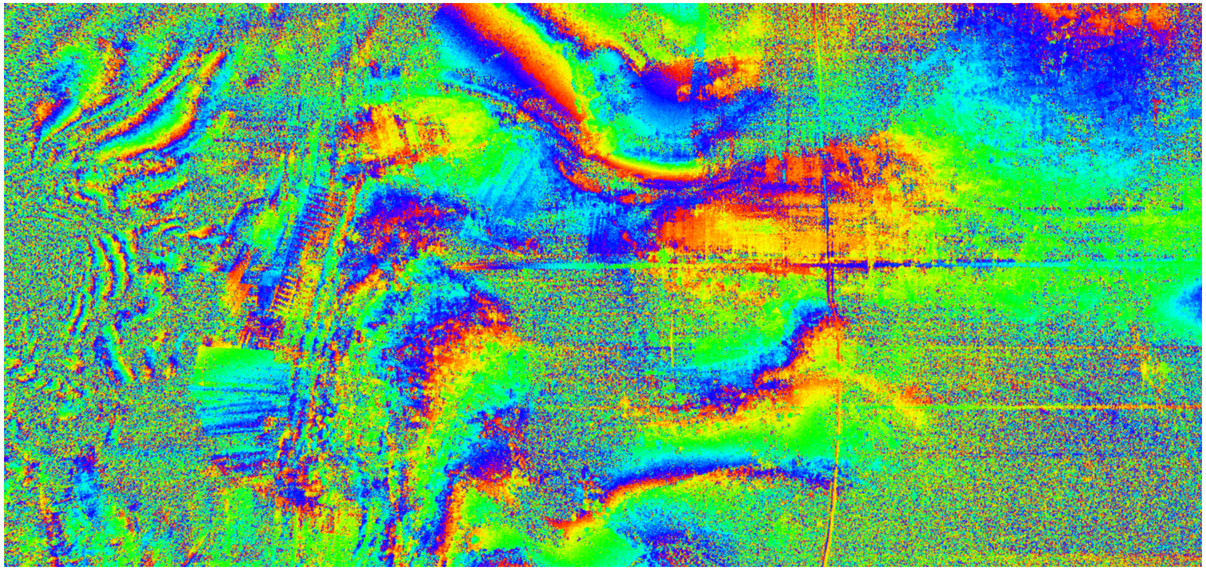

HITCHHIKER
4 Channel Extension

Single Pass Interferometry
Experiment

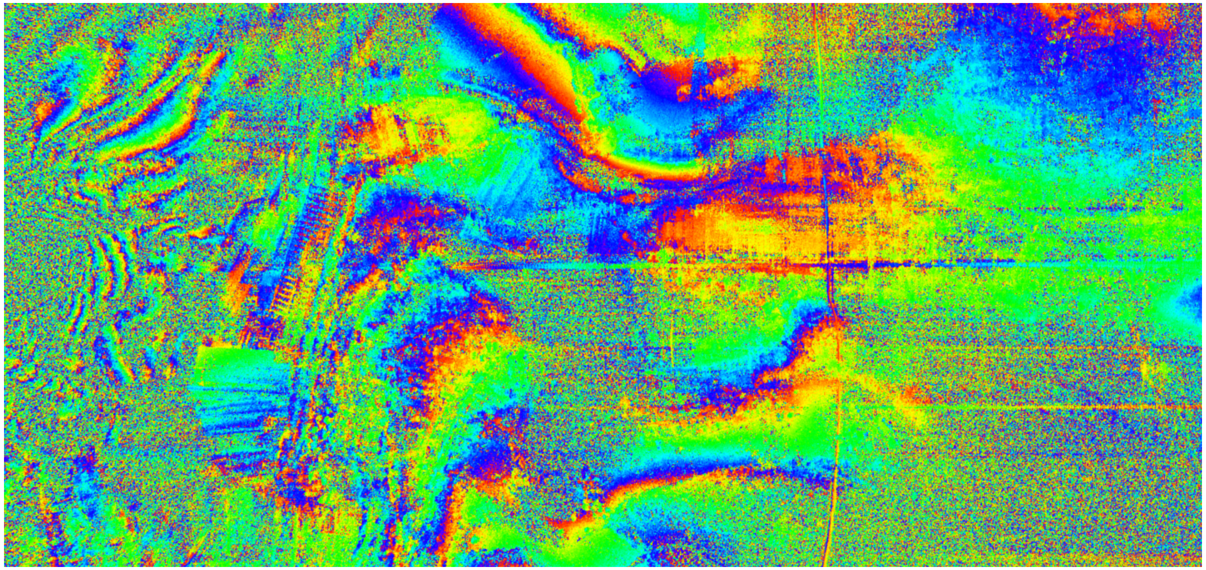

HITCHHIKER
Transmitter

HITCHHIKER
Transmitter

Indoor Noise SAR
Experiment

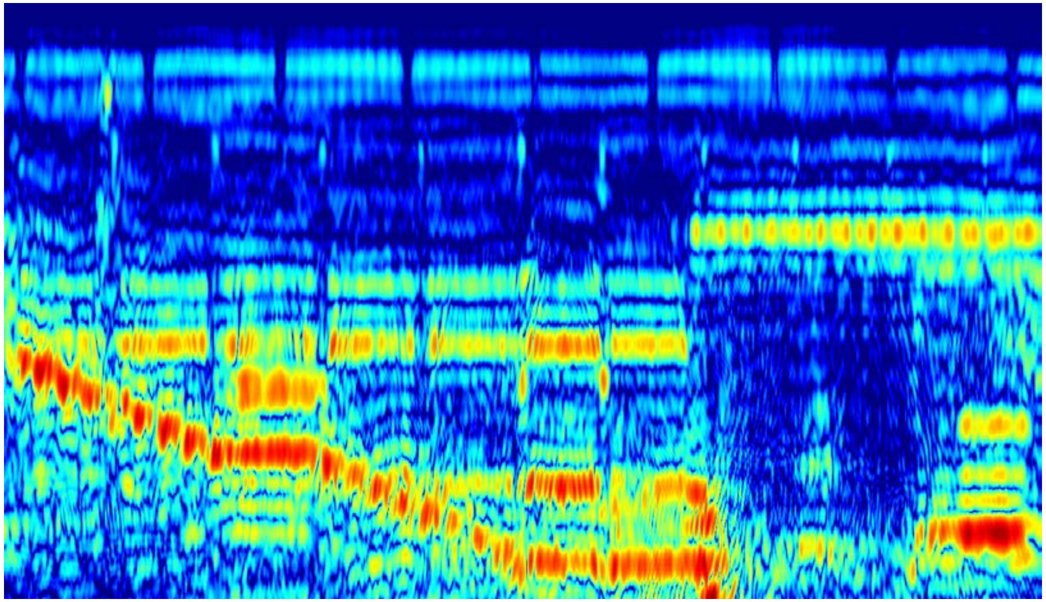

HITCHHIKER Transmitter

Indoor Noise SAR Experiment

Noise ISAR Experiment

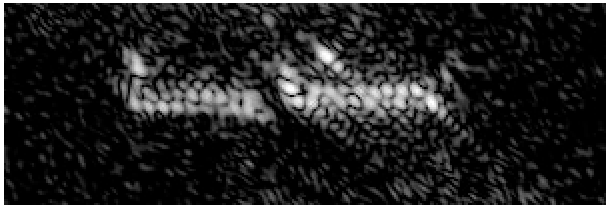

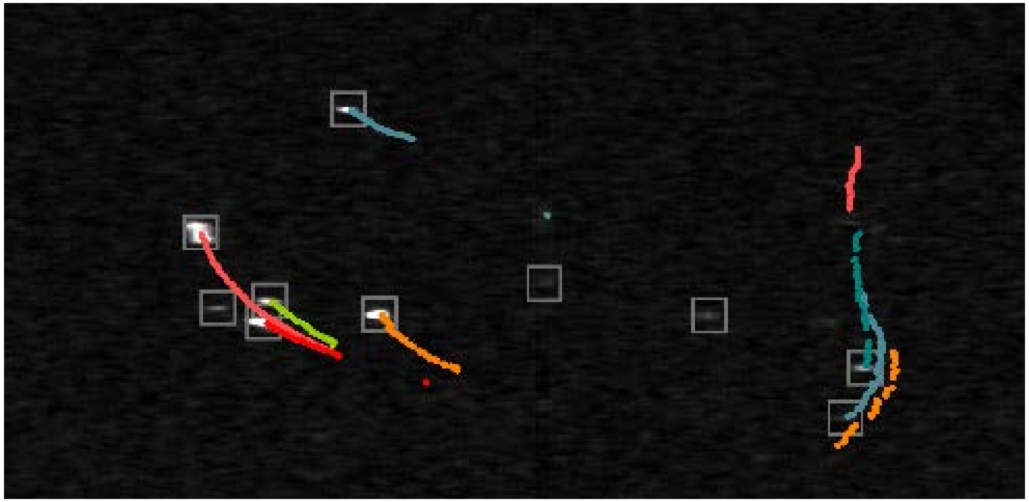

HITCHHIKER Transmitter

Indoor Noise SAR Experiment

Noise ISAR Experiment

Interferometric Antenna Setup

HITCHHIKER – TerraSAR-X
Staring Spotlight Experiment

HITCHHIKER
Transmitter

Indoor Noise SAR
Experiment

Noise ISAR
Experiment

Interferometric
Antenna Setup

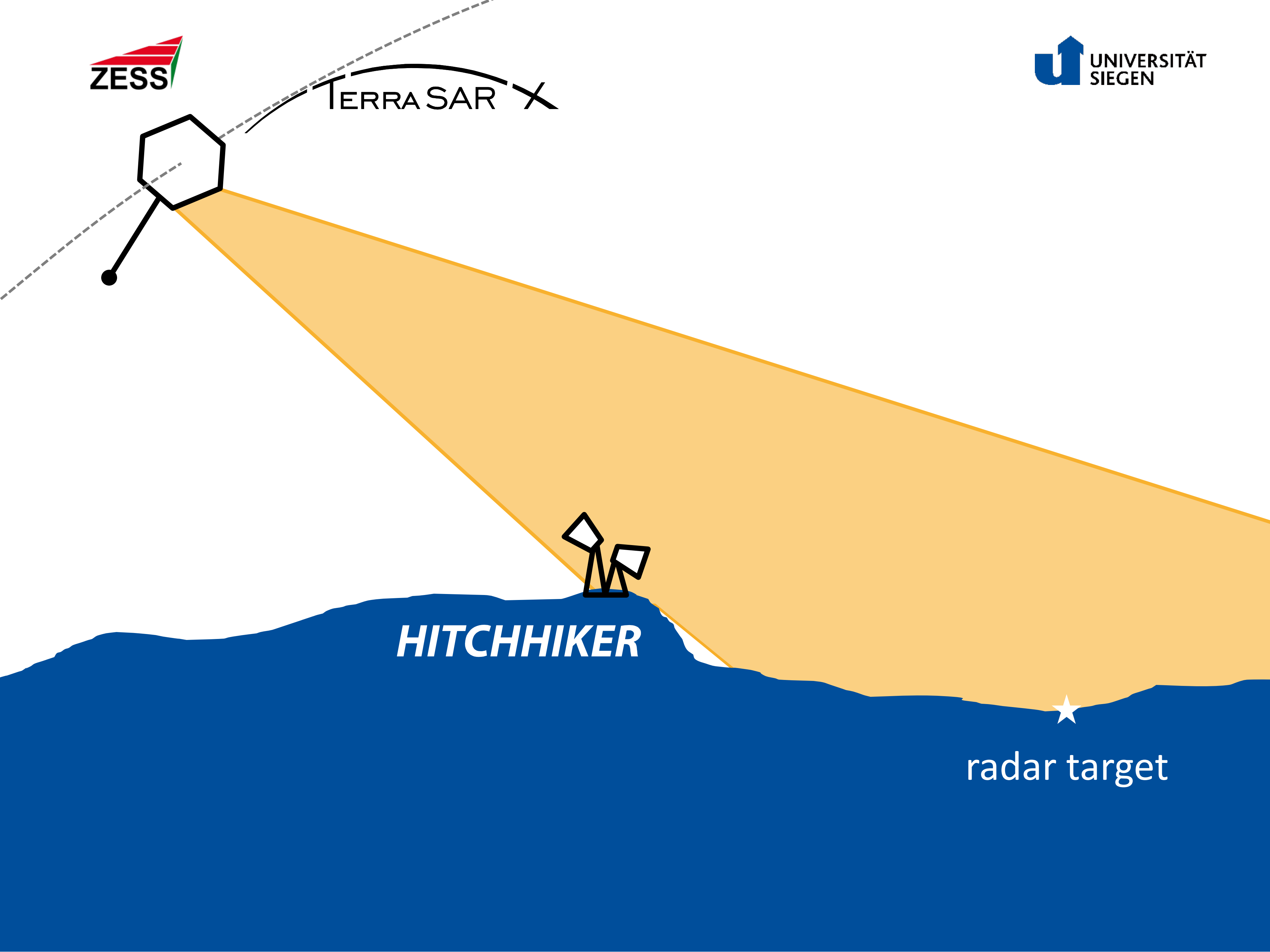
TerraSAR-X
HITCHHIKER
radar target

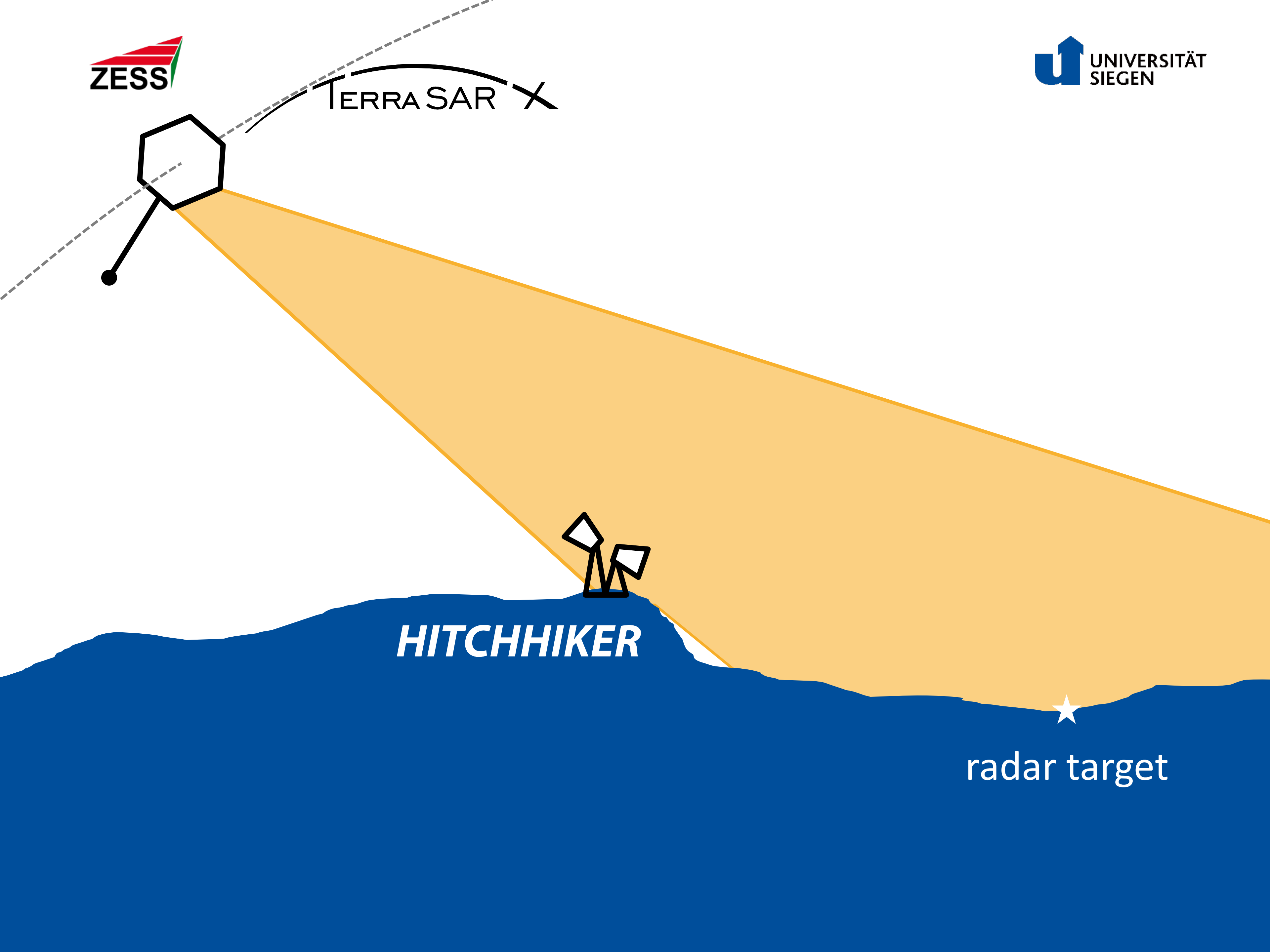
ZESS
TerraSAR-X
UNIVERSITÄT SIEGEN
HITCHHIKER
radar target

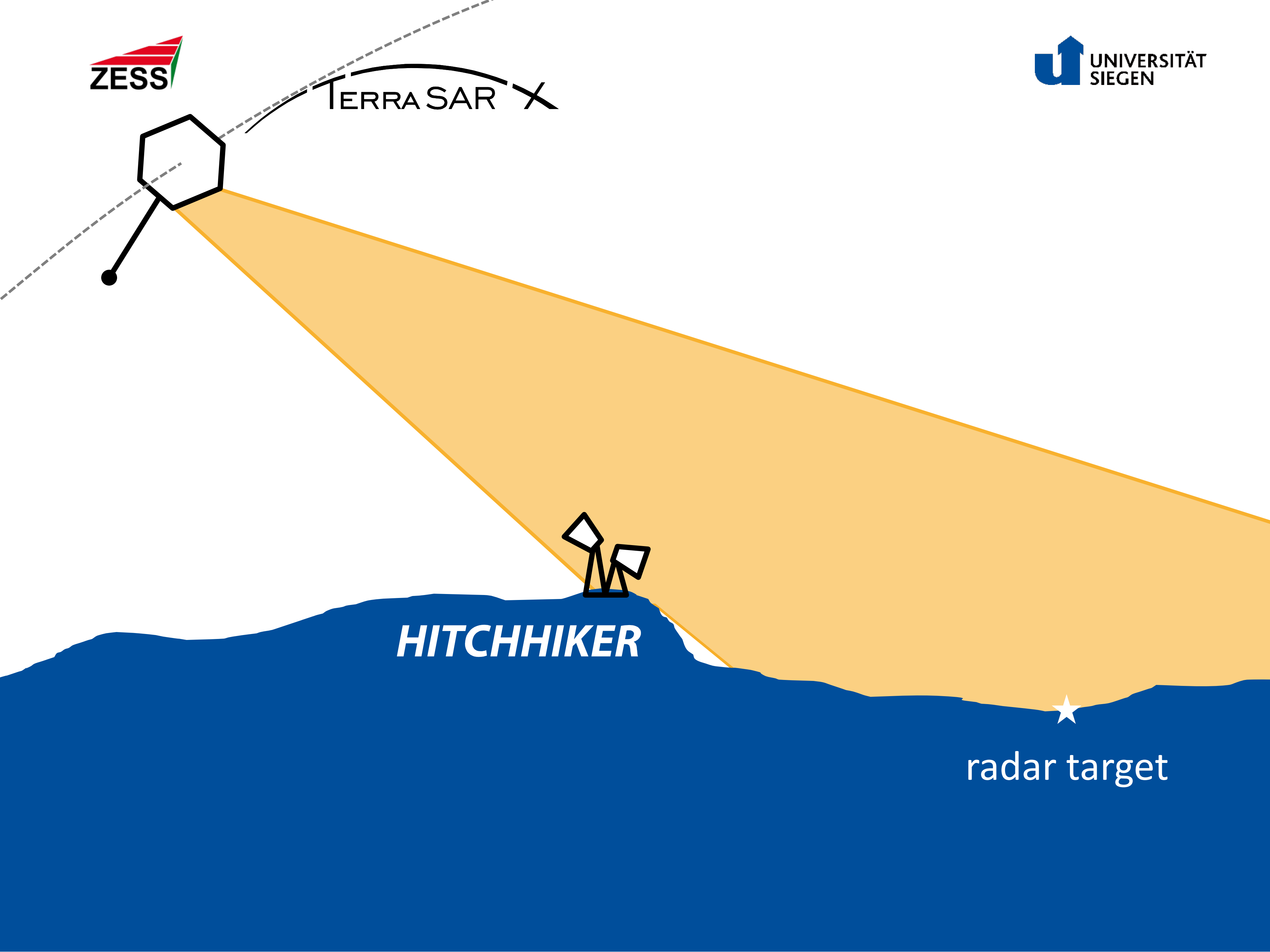
ZESS
TERRASAR-X
UNIVERSITÄT
SIEGEN
HITCHHIKER
radar target

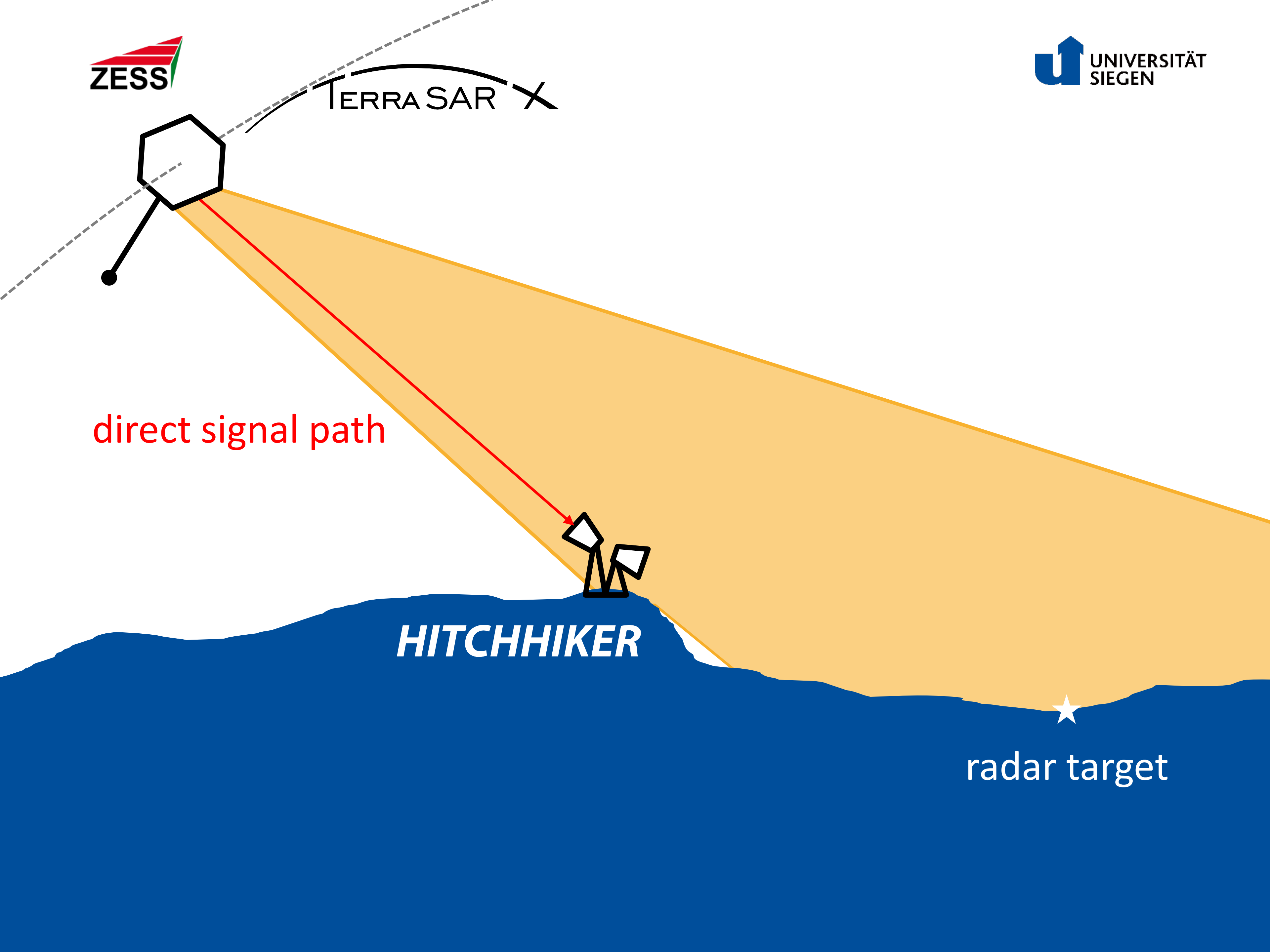
ZESS
TERRA SAR X
UNIVERSITÄT SIEGEN
direct signal path
HITCHHIKER
radar target

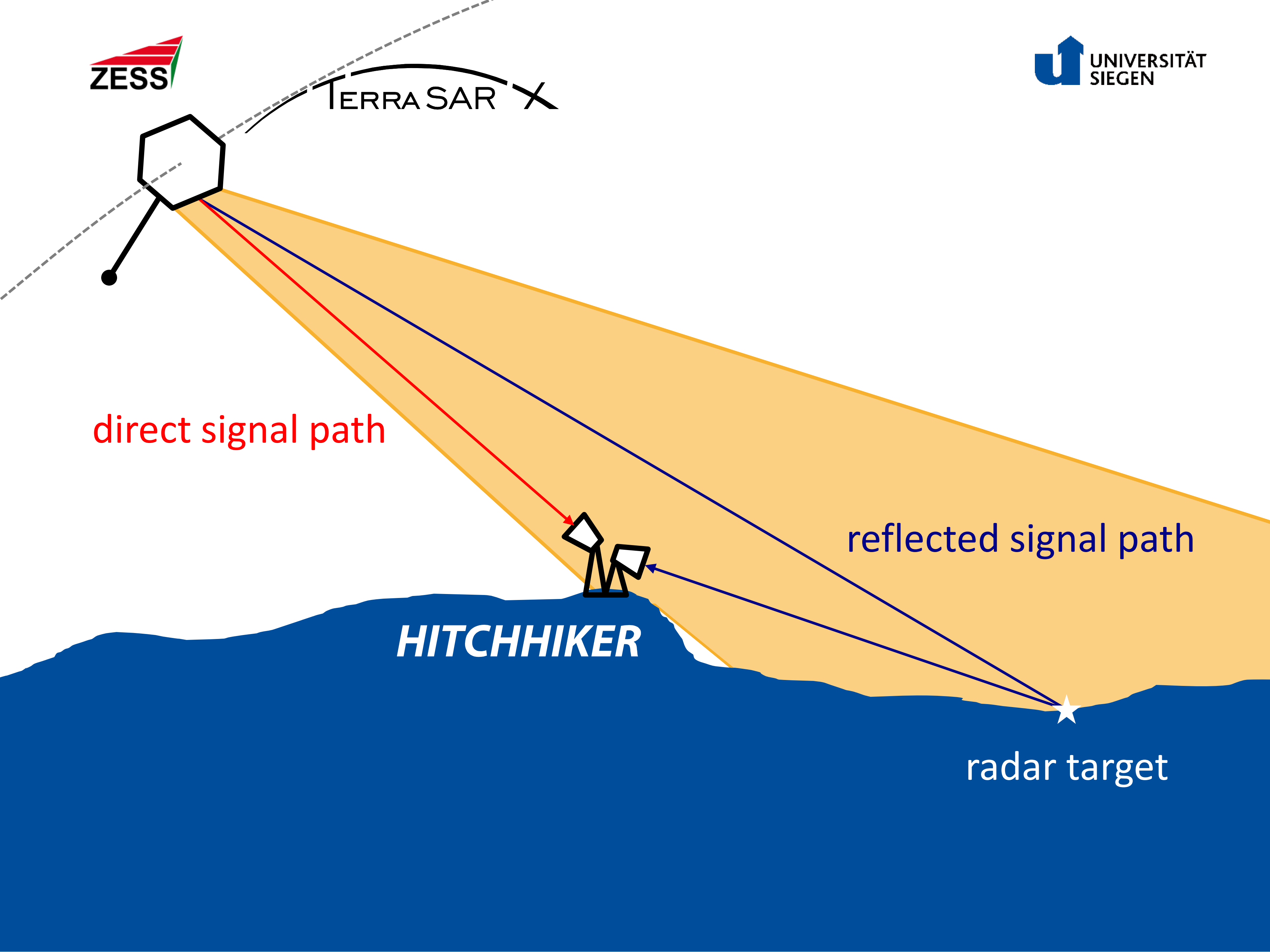
ZESS
TerraSAR-X
UNIVERSITÄT SIEGEN
direct signal path
reflected signal path
HITCHHIKER
radar target

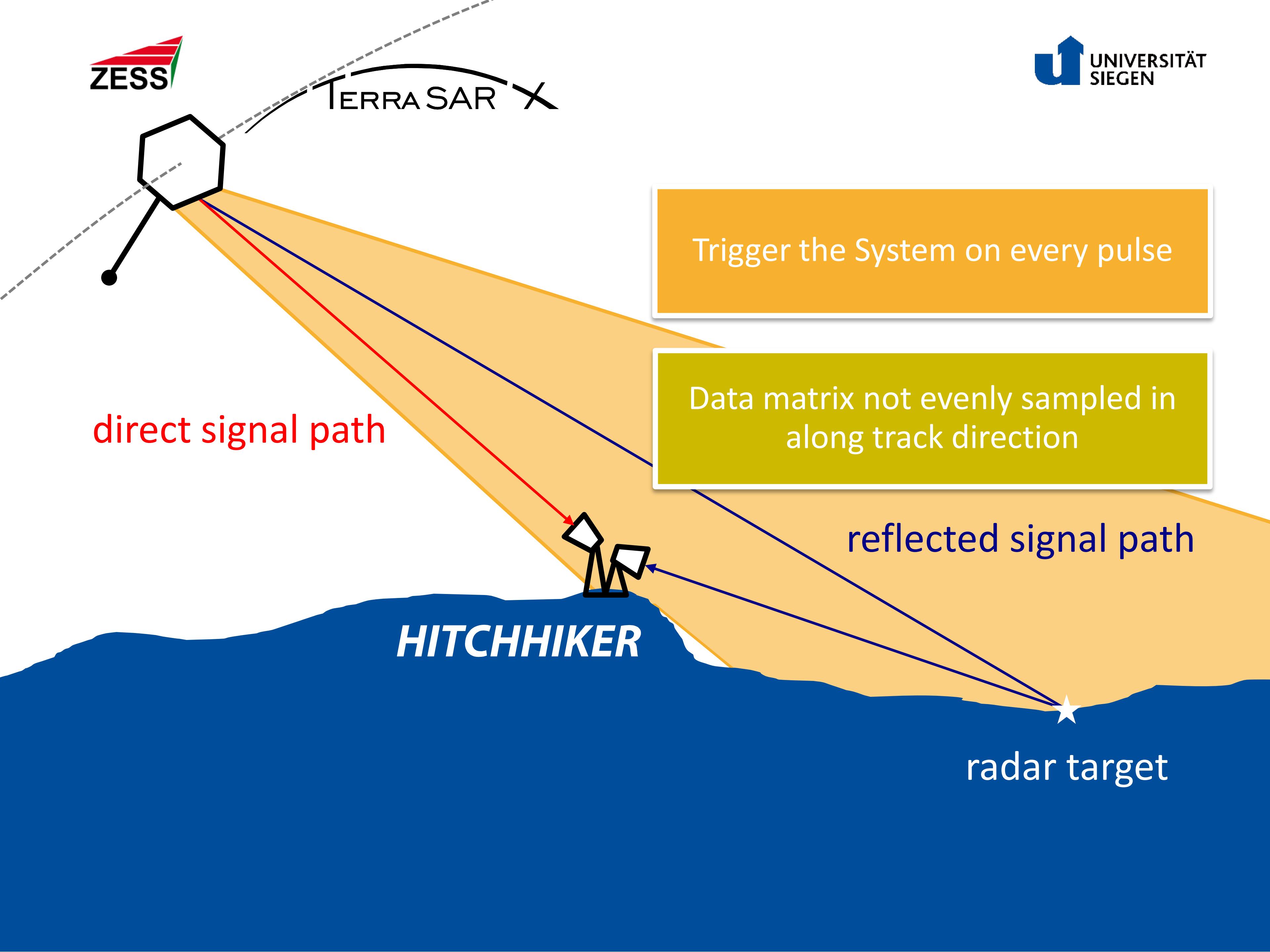
ZESS
TERRASAR-X
UNIVERSITÄT SIEGEN
Trigger the System on every pulse
Data matrix not evenly sampled in along track direction
direct signal path
reflected signal path
HITCHHIKER
radar target

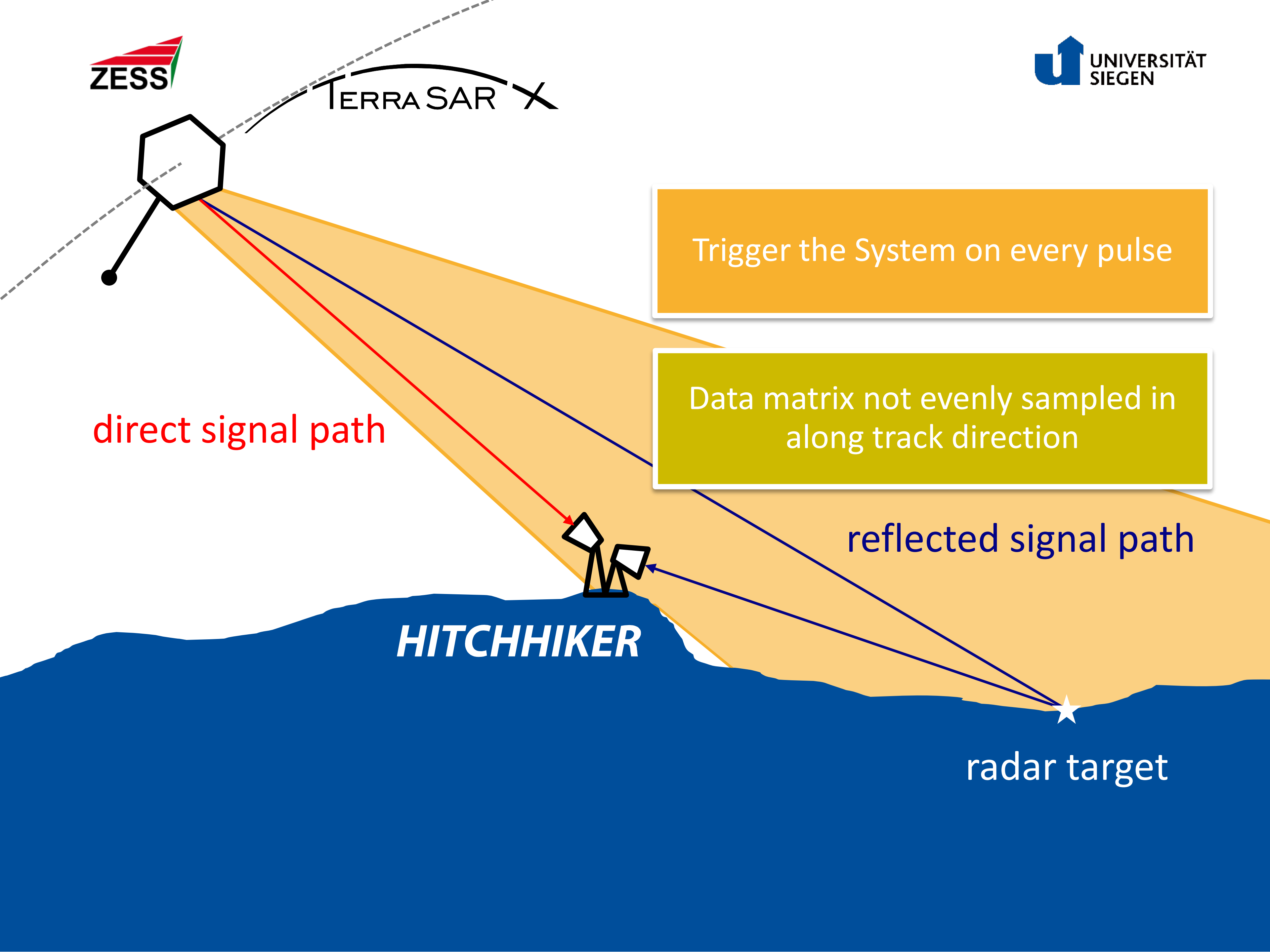
ZESS
TERRASAR-X
UNIVERSITÄT SIEGEN
Trigger the System on every pulse
Data matrix not evenly sampled in along track direction
direct signal path
reflected signal path
HITCHHIKER
radar target

Receiver hardware synchronization

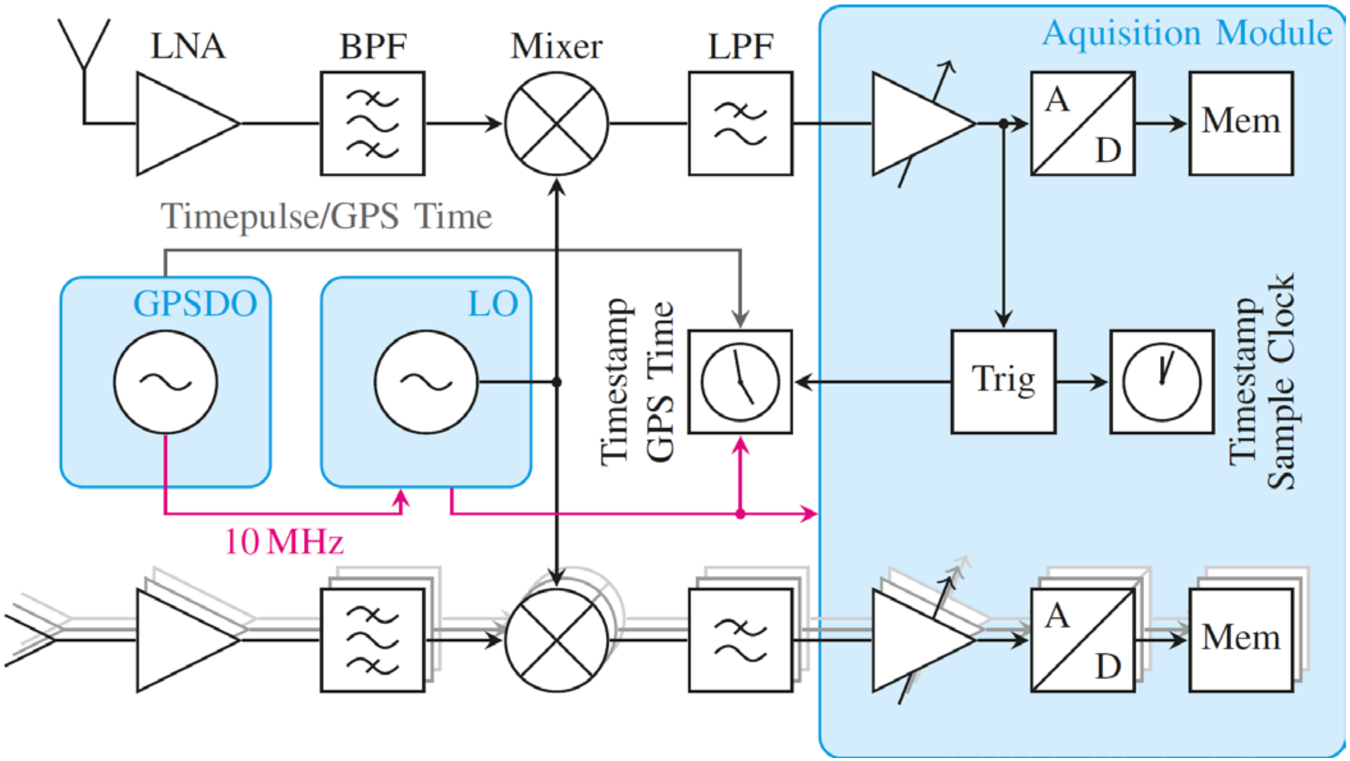

Processing framework

- Processing block implemented as Matlab class
  - parameters, input, output
  - Versioning and recursive validity check of data
- Use HDF 5 files as interface between blocks

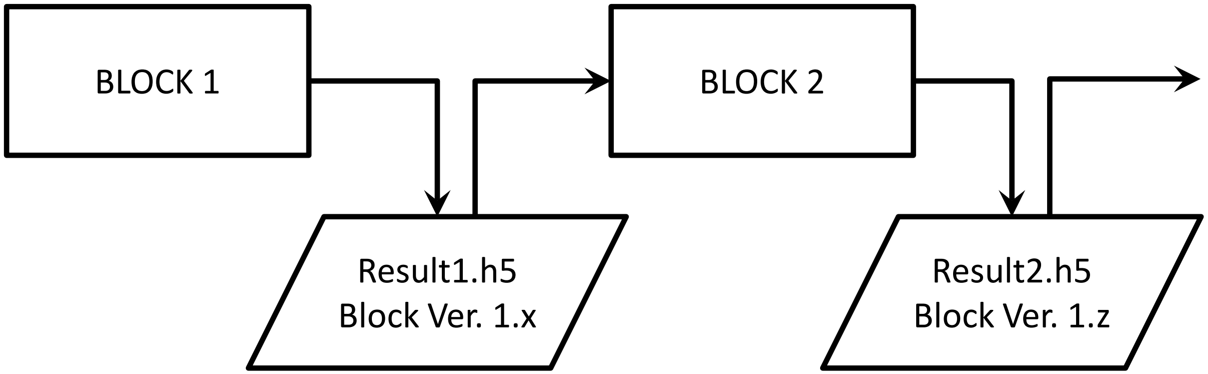

Baseband conversion

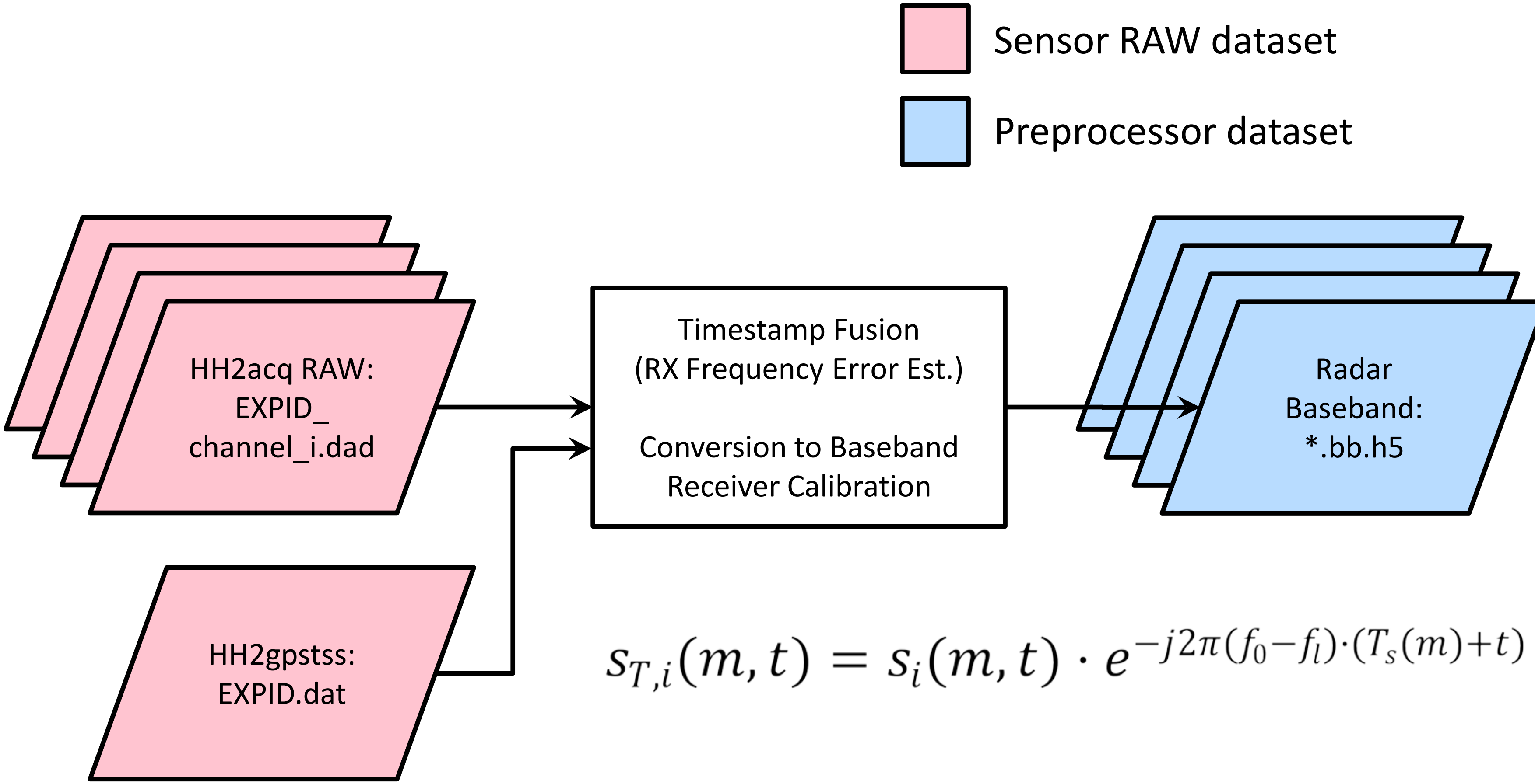

$$s_{T,i}(m,t) = s_i(m,t) \cdot e^{-j2\pi(f_0 - f_l)\cdot(T_s(m)+t)}$$

Baseband conversion and channel equalization

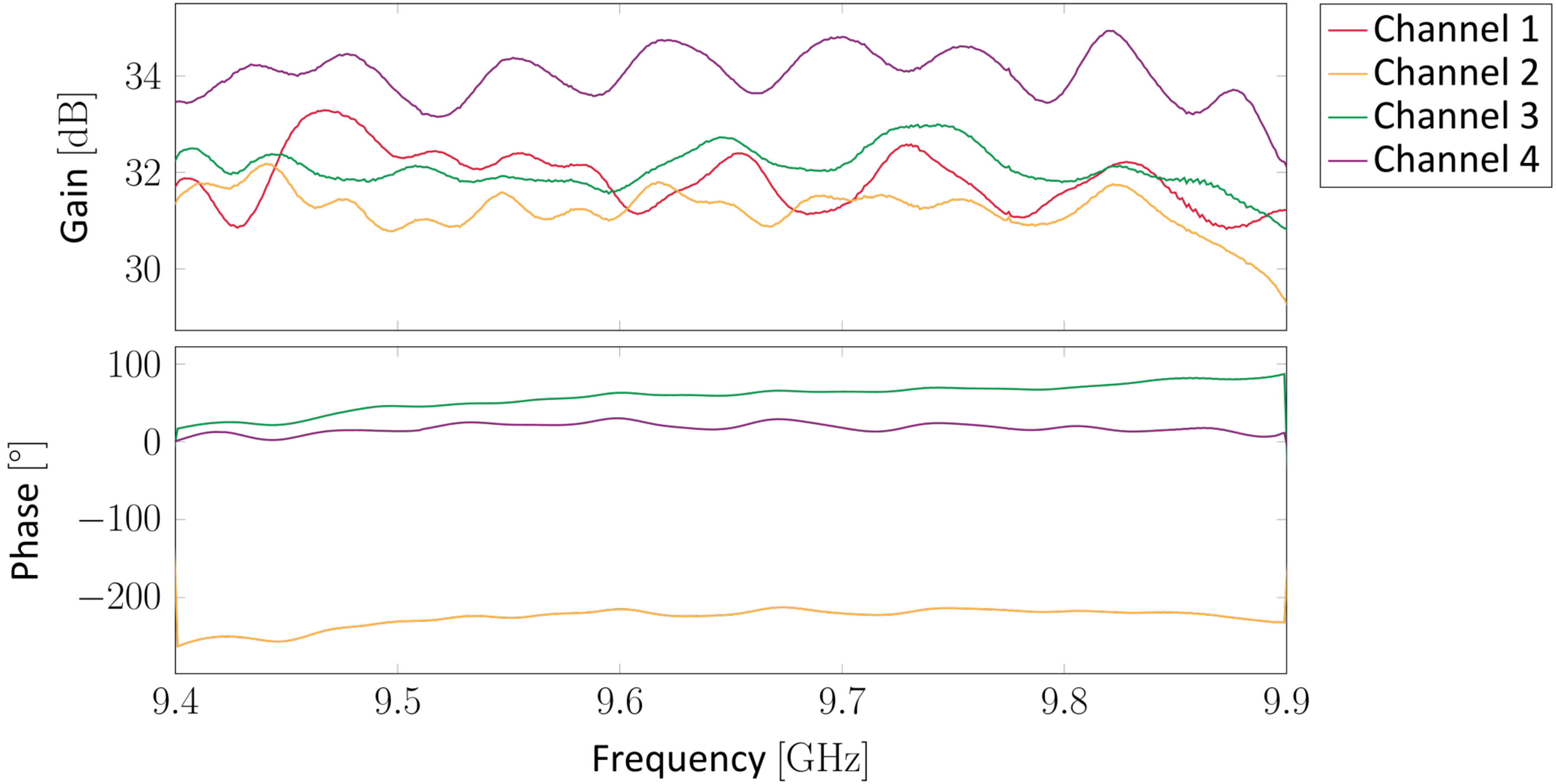

Analysis of the reference signal

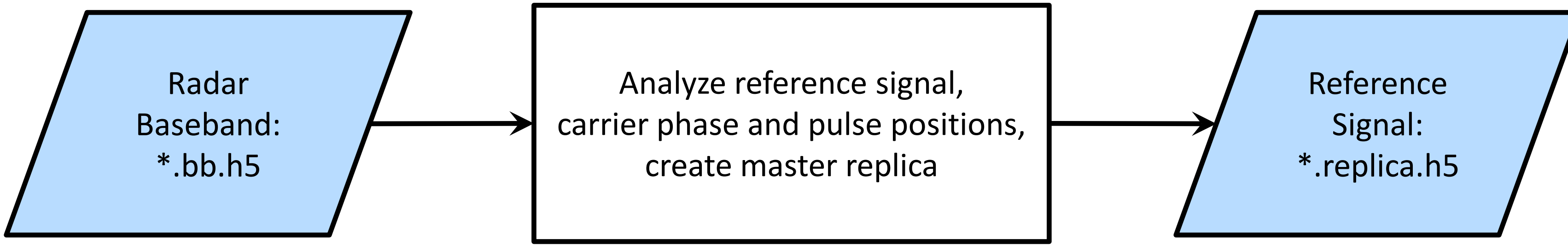

Analysis of the reference signal

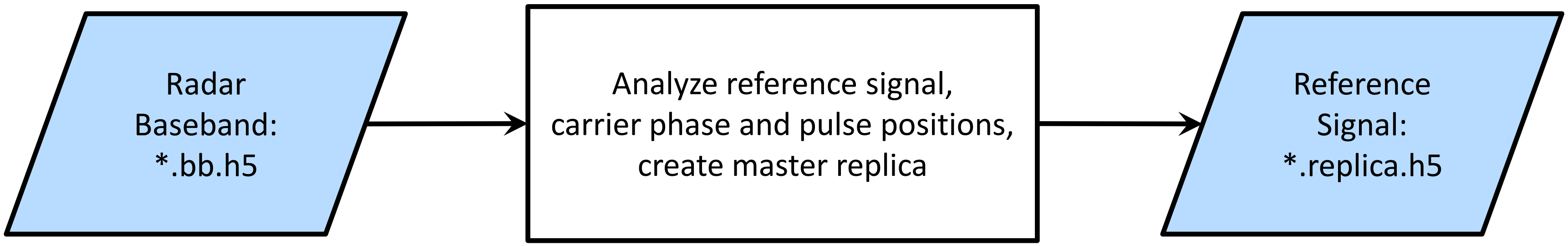

$$s_d(m,t) = s_T(t - (\tau(m) - T_d(m))) \cdot e^{j2\pi(f_0^{'} - f_0)\cdot(t + T_s(m))} \cdot e^{-j2\pi f_0^{'} \tau(m)}$$

$$T_d(m) = T_s(m) - (T_0 + Z(m) \cdot T_i)$$

Analysis of the reference signal

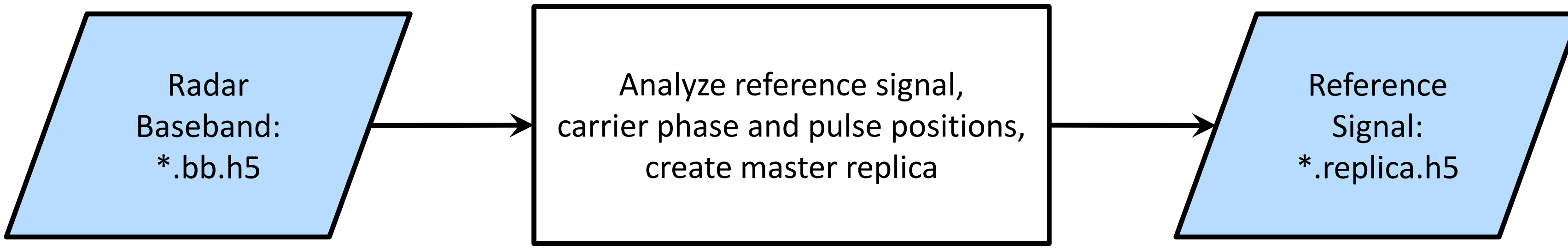

$$s_d(m,t) = s_T(t - (\tau(m) - T_d(m))) \cdot e^{j2\pi(f_0' - f_0)\cdot(t + T_s(m))} \cdot e^{-j2\pi f_0' \tau(m)}$$

$$T_d(m) = T_s(m) - (T_0 + Z(m) \cdot T_i)$$

$$S_d(m,f) = \left(S_T(f) \cdot e^{-j2\pi f(\tau(m) - T_d(m))} \cdot e^{j2\pi(f_0' - f_0)\cdot T_s(m)} \cdot e^{-j2\pi f_0' \tau(m)}\right) * \delta(f - (f_0' - f_0))$$

Analysis of the reference signal

$$\angle S_d(m,f)\cdot S_d^*(M,f) = 2\pi f\left(T_d(m)-T_d(M)\right) - 2\pi f\left(\tau(m)-\tau(M)\right)$$
$$- 2\pi f_0\left(\tau(m)-\tau(M)\right)$$
$$+ 2\pi\left(f_0^{'}-f_0\right)\left(Z(m)-Z(M)\right)\cdot T_i$$

Analysis of the reference signal

$$\begin{aligned}\angle S_d(m,f)\cdot S_d^*(M,f) &= 2\pi f(T_d(m)-T_d(M)) - 2\pi f(\tau(m)-\tau(M))\\ &\quad - 2\pi f_0(\tau(m)-\tau(M))\\ &\quad + 2\pi(f_0^{'}-f_0)(Z(m)-Z(M))\cdot T_i\end{aligned}$$

$$\begin{aligned}\Delta T(m) &= -\frac{1}{2\pi}\frac{\mathrm{d}}{\mathrm{d}f}\angle S_d(m,f)\cdot S_d^*(M,f)\\ &= \tau(m)-\tau(M)\\ &\quad -(T_d(m)-T_d(M))\end{aligned}$$

Analysis of the reference signal

$$\angle S_d(m,f)\cdot S_d^*(M,f) = 2\pi f(T_d(m)-T_d(M)) - 2\pi f(\tau(m)-\tau(M))$$
$$-\ 2\pi f_0(\tau(m)-\tau(M))$$
$$+\ 2\pi(f_0^{'}-f_0)(Z(m)-Z(M))\cdot T_i$$

$$\Delta T(m) = -\frac{1}{2\pi}\frac{\mathrm{d}}{\mathrm{d}f}\angle S_d(m,f)\cdot S_d^*(M,f)$$
$$= \tau(m)-\tau(M)$$
$$-\ (T_d(m)-T_d(M))$$

$$\varphi_T(m) = \angle S_d(m,f)\cdot S_d^*(M,f)|_{f=0}$$
$$= 2\pi(f_0^{'}-f_0)(Z(m)-Z(M))\cdot T_i$$
$$-\ 2\pi f_0(\tau(m)-\tau(M))$$

Calculation of the replica

$$S_T'(f) = \sum_m S_d(m,f) \cdot e^{j2\pi f \Delta T(m)} e^{-j\varphi_T(m)}$$

$$= C \cdot S_T(f - (f_0' - f_0)) e^{-j2\pi f(\tau(M) - T_d(M))}$$

$$\cdot e^{j2\pi(f_0' - f_0)Z(M)\cdot T_i} e^{-j2\pi f_0 \tau(M))}$$

Calculation of the replica

$$S_T'(f) = \sum_m S_d(m,f) \cdot e^{j2\pi f \Delta T(m)} e^{-j\varphi_T(m)}$$

$$= C \cdot S_T(f - (f_0' - f_0)) e^{-j2\pi f(\tau(M) - T_d(M))}$$

$$\cdot\, e^{j2\pi(f_0' - f_0) Z(M) \cdot T_i} e^{-j2\pi f_0 \tau(M))}$$

Correct relative delay and phase to reference pulse M

Integrate over all completely received pulses

Calculation of the replica

$$S_T'(f) = \sum_m S_d(m,f) \cdot e^{j2\pi f \Delta T(m)} e^{-j\varphi_T(m)}$$
$$= C \cdot S_T(f - (f_0' - f_0)) e^{-j2\pi f(\tau(M) - T_d(M))}$$
$$\cdot\, e^{j2\pi(f_0' - f_0)Z(M)\cdot T_i} e^{-j2\pi f_0 \tau(M))}$$

Correct relative delay and phase to reference pulse M

Integrate over all completely received pulses

$$T_r(m) = T_s(m) + \Delta T(m)$$

TerraSAR-X Signal

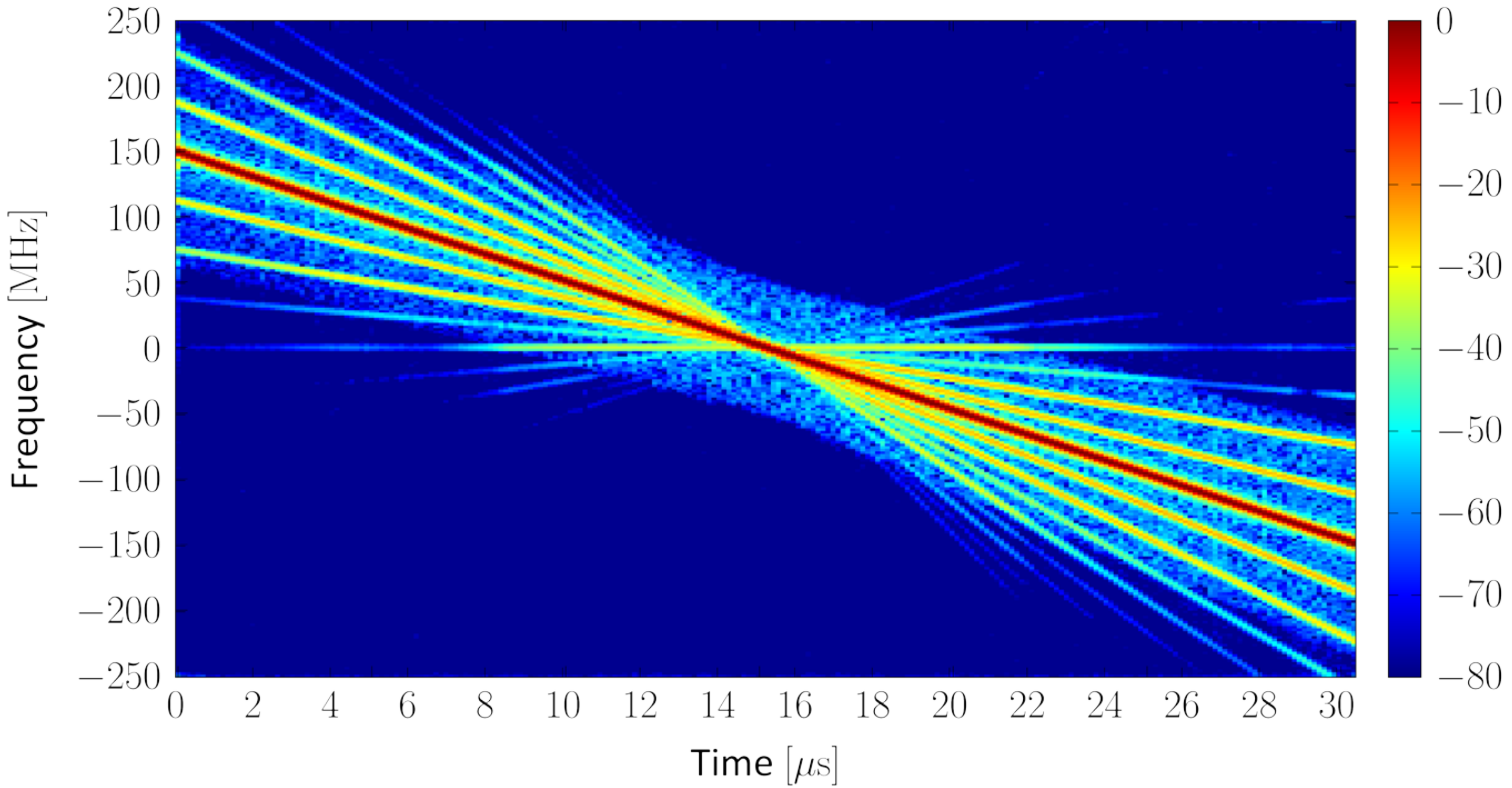

TanDEM-X Signal

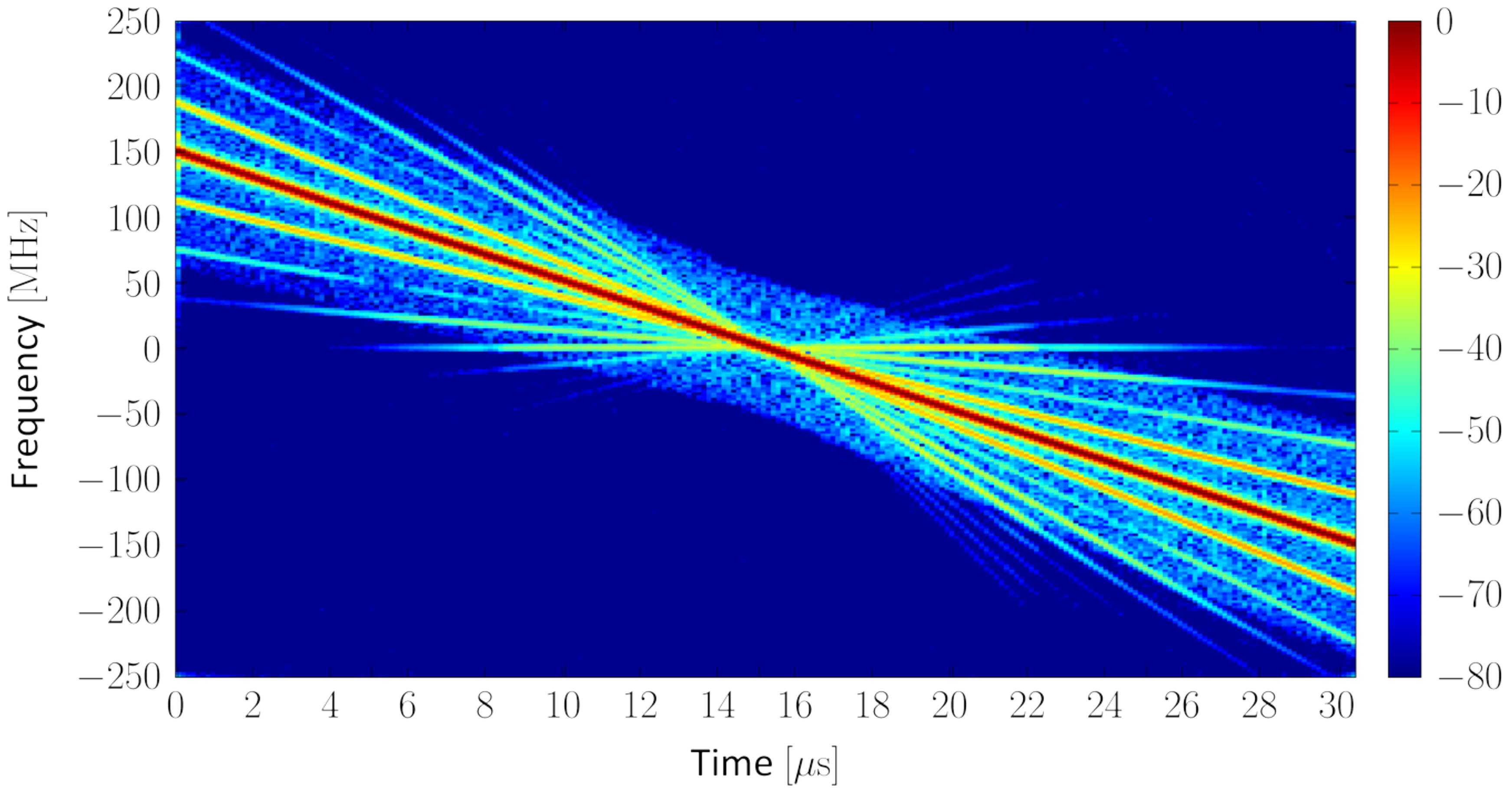

Bistatic SAR Image Formation

Bistatic Geometry
Resolution

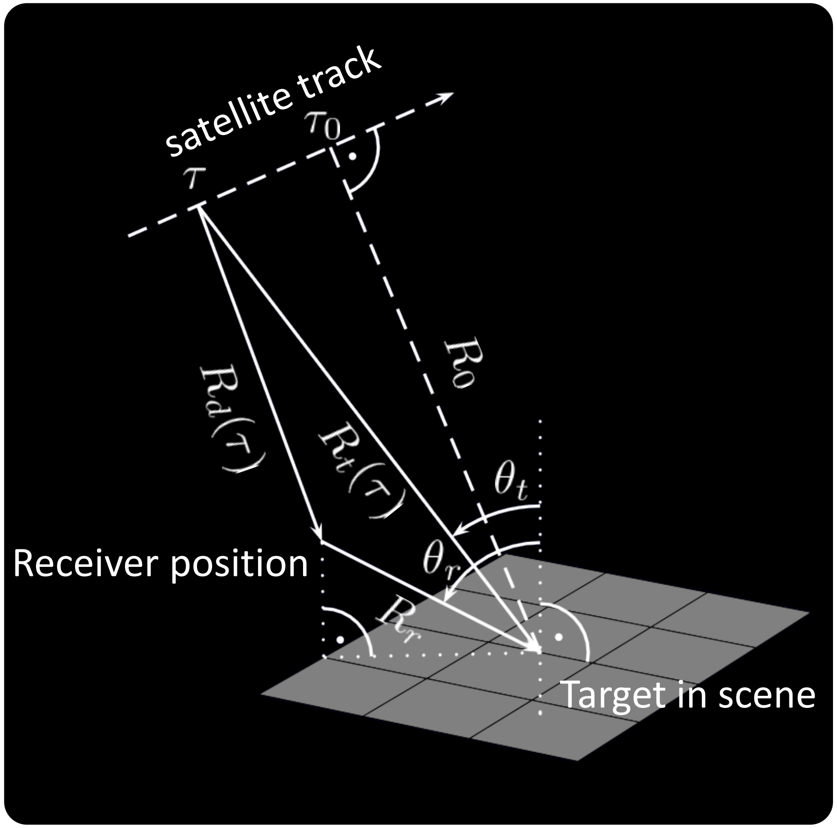

Across-Track Resolution

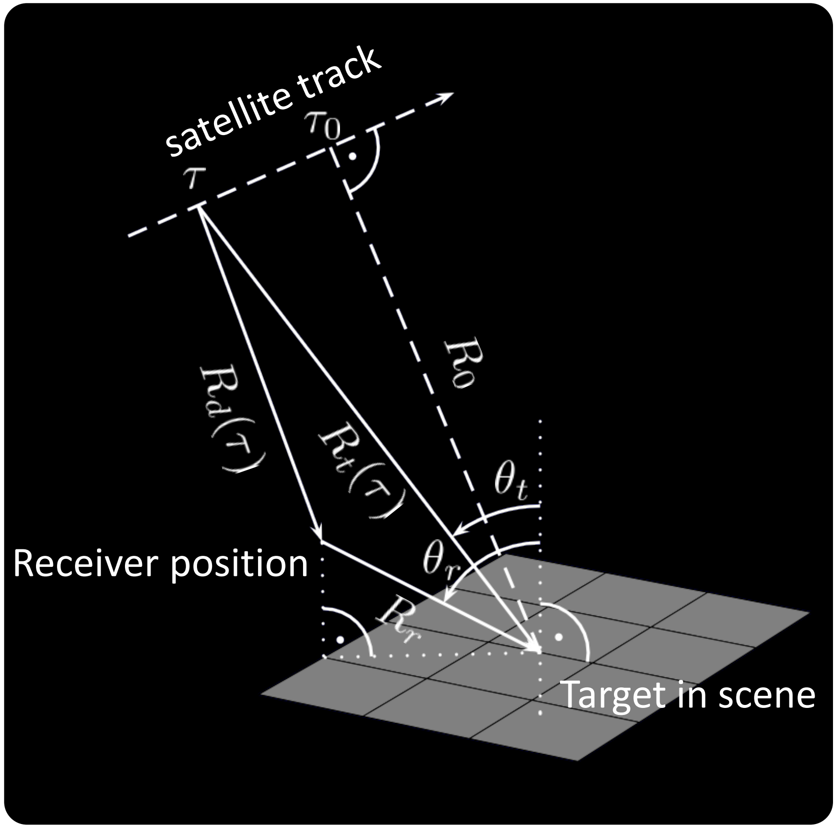

$$\delta_c = \frac{c}{B \cdot (\sin\theta_t + \sin\theta_r)}$$

Bistatic Geometry
Resolution

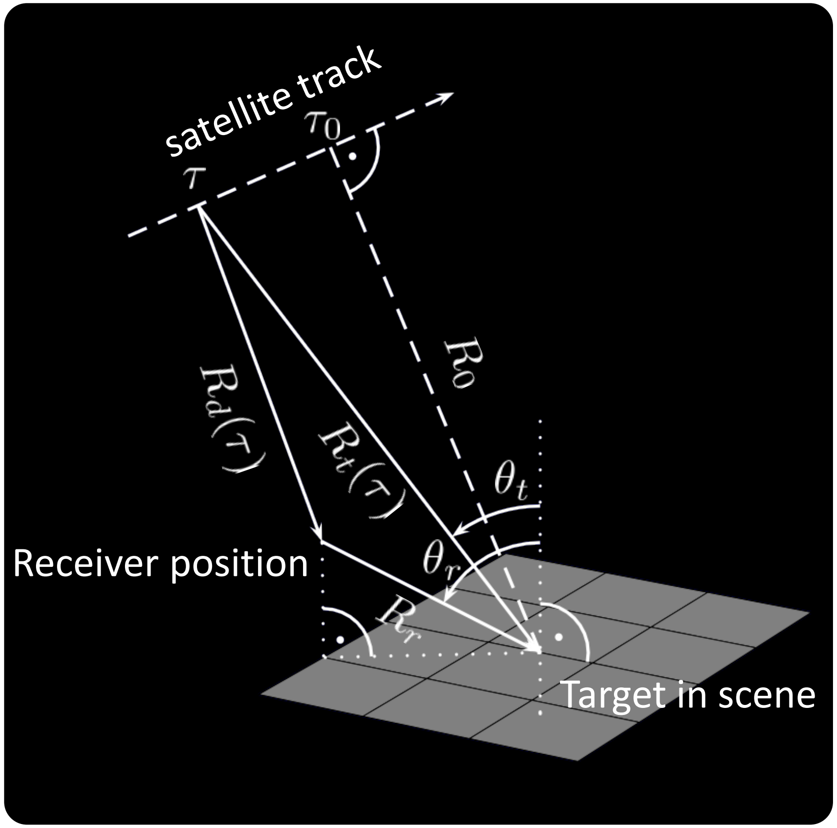

Across-Track Resolution

$$\delta_c = \frac{c}{B \cdot (\sin\theta_t + \sin\theta_r)}$$

Along-Track Resolution

$$\delta_a = \frac{\lambda_0}{2}\sqrt{\frac{4R_0^2}{(v \cdot T_i)^2} + 1}$$

Bistatic Geometry

Resolution

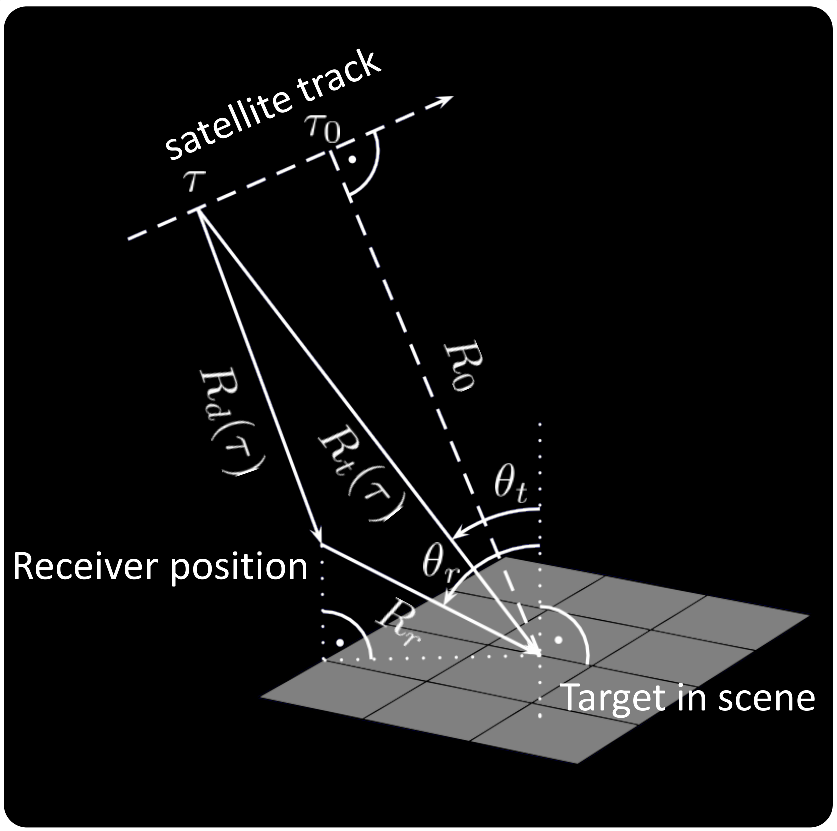

Across-Track Resolution

$$\delta_c = \frac{c}{B \cdot (\sin\theta_t + \sin\theta_r)}$$

Along-Track Resolution

$$\delta_a = \frac{\lambda_0}{2}\sqrt{\frac{4R_0^2}{(v \cdot T_i)^2} + 1}$$

λ_0: wavelength
R_0: min. range target - transmitter
v: transmitter's velocity
T_i: illumination time

Bistatic Geometry

Iso-range and iso-doppler contours

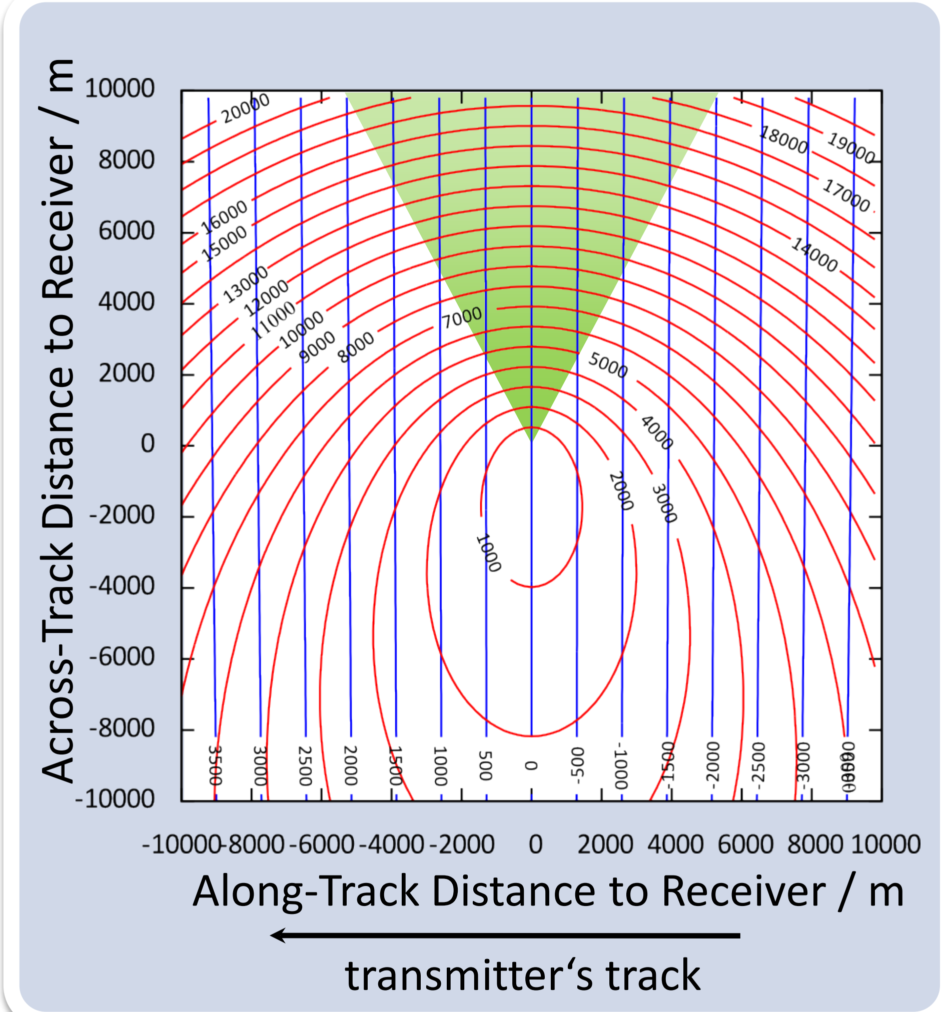

Bistatic Geometry
Iso-range and iso-doppler contours

Across-track resolution:

0.56 m

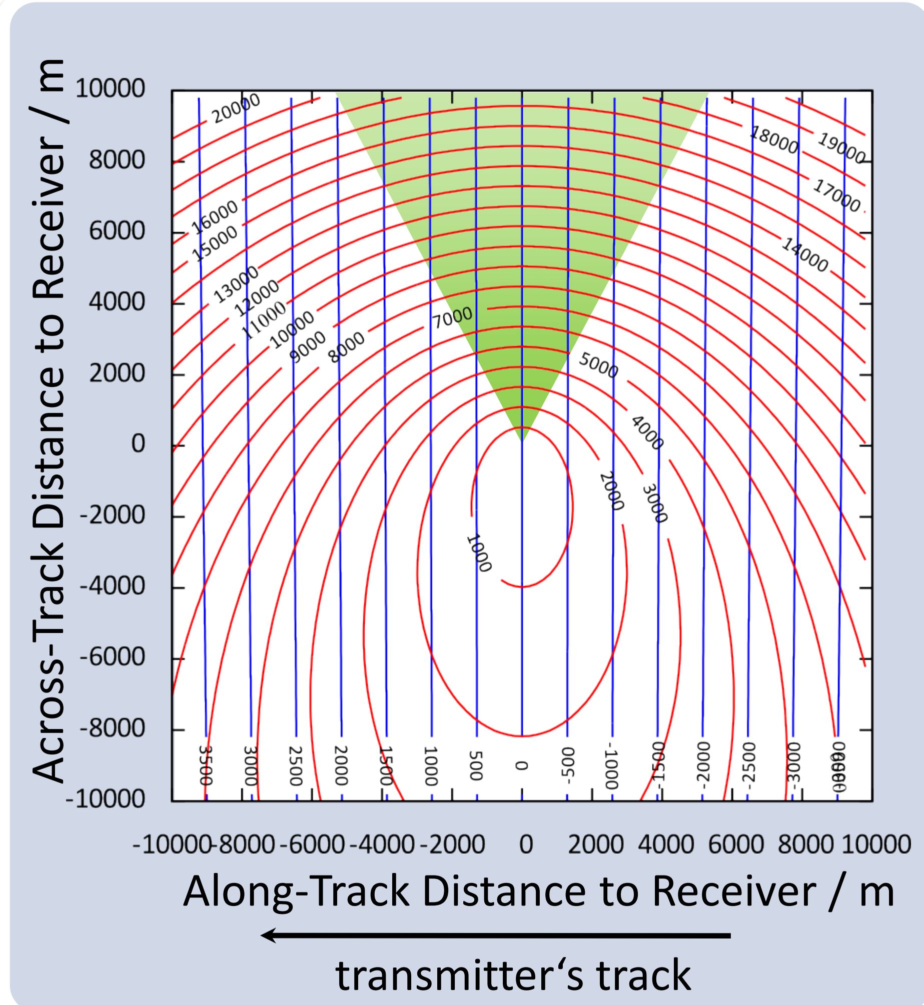

Bistatic Geometry

Iso-range and iso-doppler contours

Across-track resolution:

0.56 m

Along-track resolution (HS mode):

1.40 m

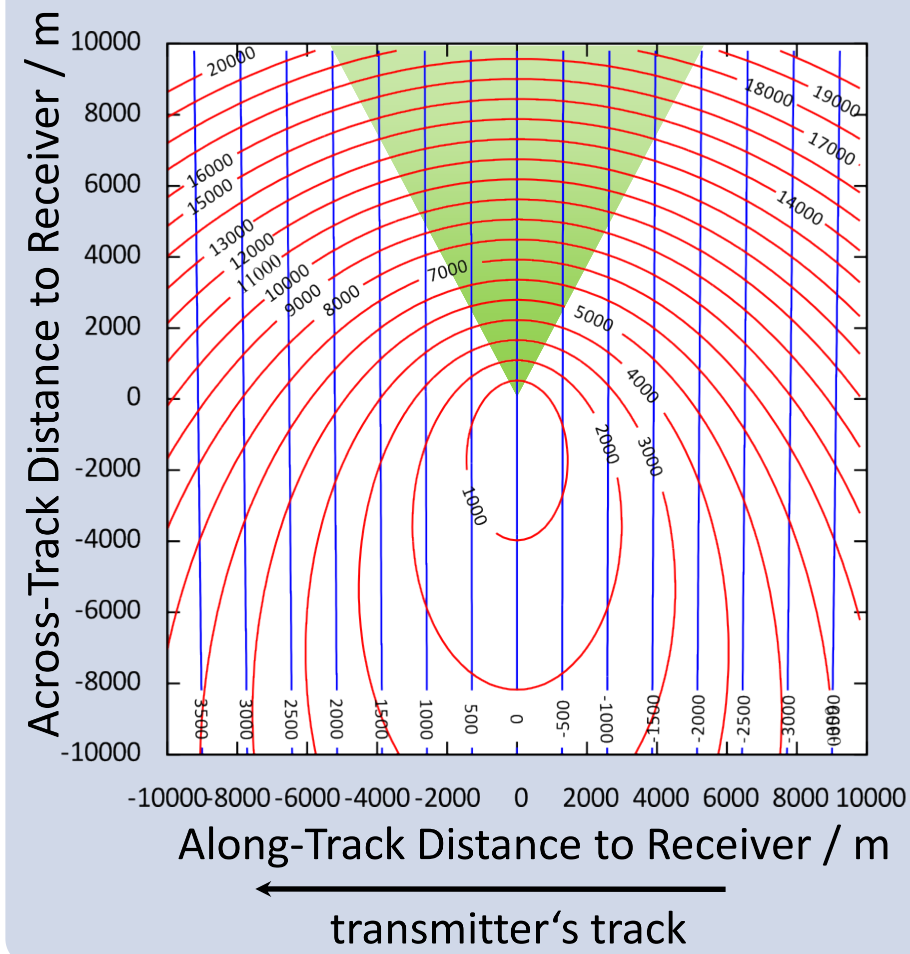

Bistatic Geometry

Iso-range and iso-doppler contours

Across-track resolution:

0.56 m

Along-track resolution (HS mode):

1.40 m

Best resolution is achieved when transmitter and receiver are looking into the same direction

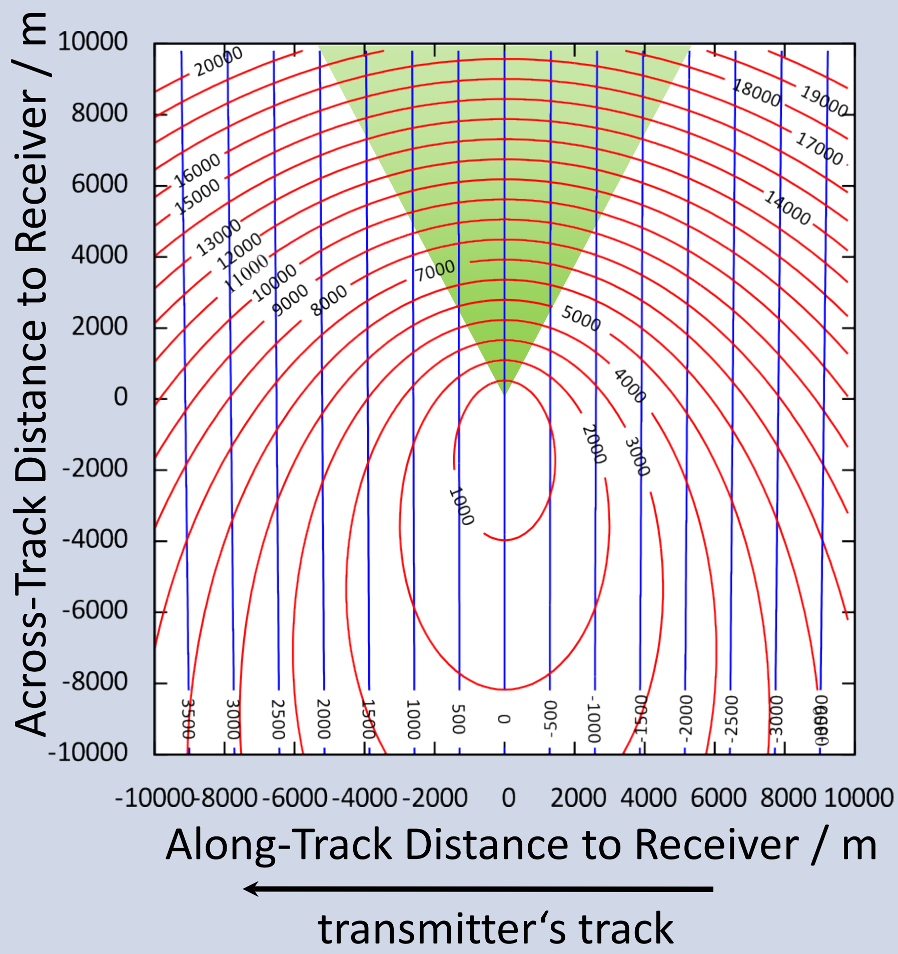

Image Formation

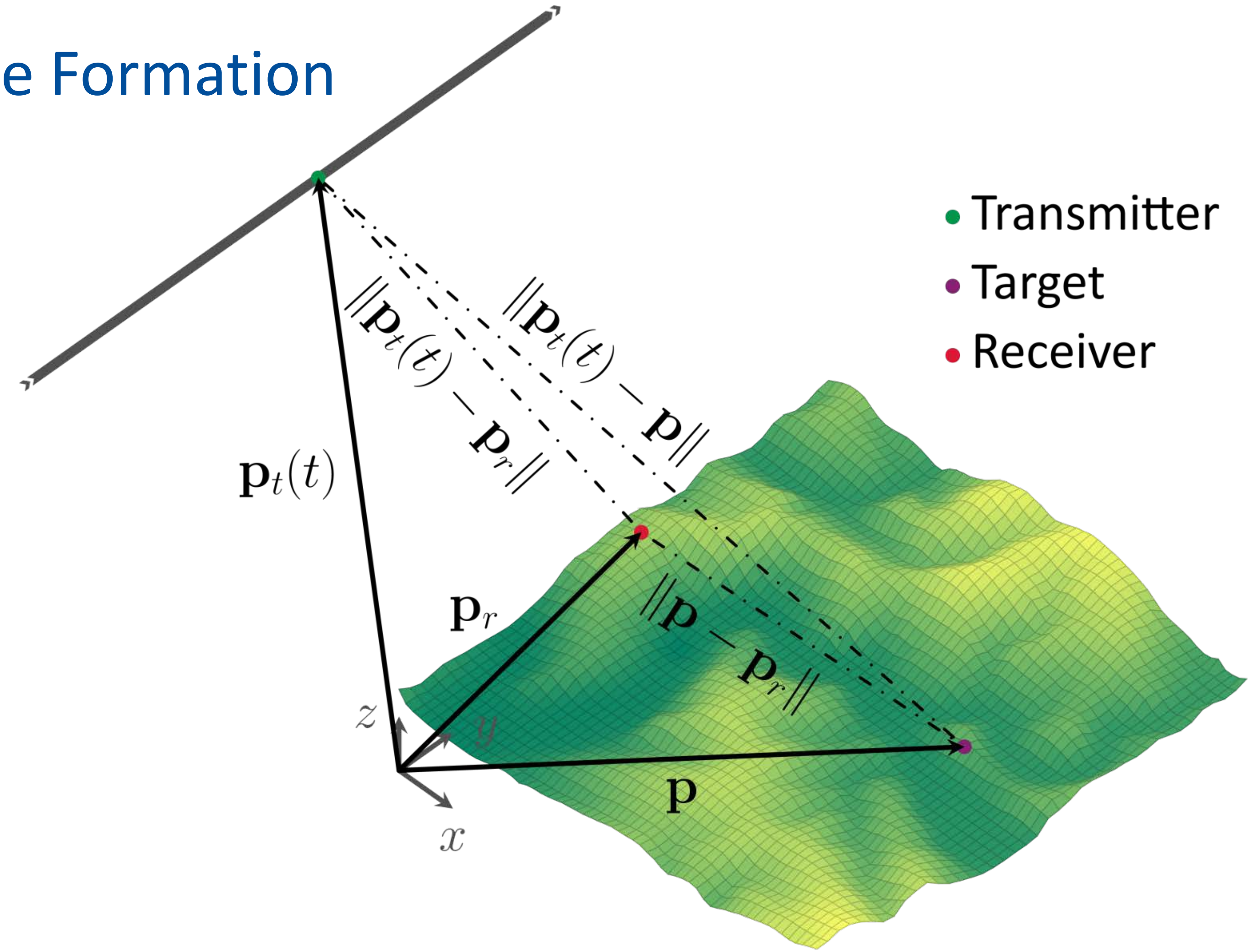

- Transmitter
- Target
- Receiver

SAR Image Formation on GPU

Nvidia GeForce	GTX 670	GTX 980 Ti	GTX 1080
Radar Signal Size	147 MS	207 MS	?
SAR Image Size	209 MP	294 MP	?
Processing Speed	80 kP/s	160 kP/s	?
SP Compute Power	2460 GFlops	5632 GFlops	8228 GFlops
GPU Memory	2 GiB	6 GiB	8 GiB
Release Price / Year	$400 / 2012	$649 / 2015	$599 / 2016

[1] F. Behner, S. Reuter, H. Nies and O. Loffeld (2016, Mar.). Synchronization and Processing in the HITCHHIKER Bistatic SAR Experiment. *IEEE Journal of Selected Topics in Applied Earth Observations and Remote Sensing*, vol. 9, no. 3, pp. 1028-1035.

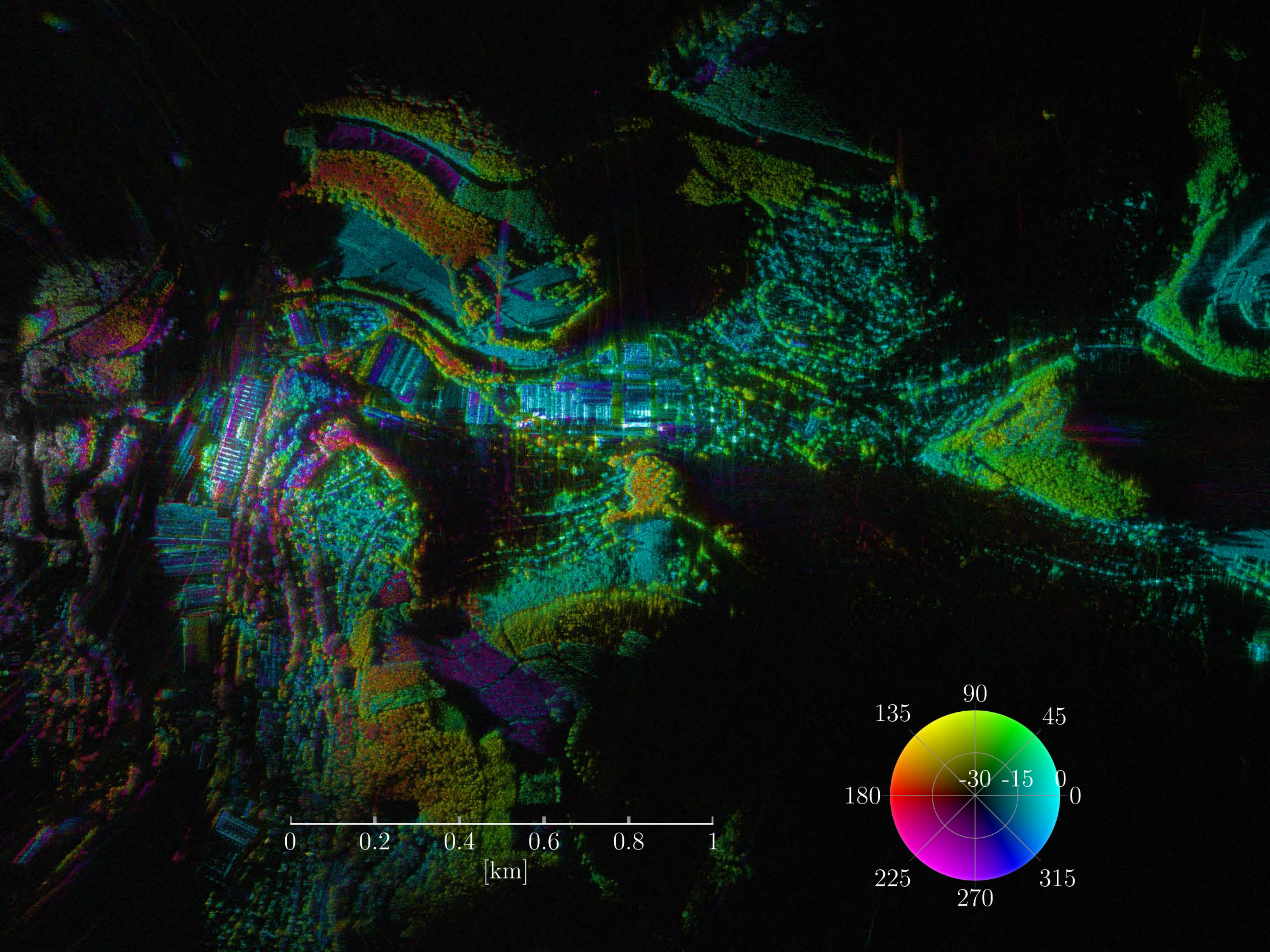

0
0.2
0.4
0.6
0.8
1
[km]
90
135
45
180
-30
-15
0
0
225
270
315

Bistatic Radar Coordinates

The bistatic radar coordinate system is a non-linear and surjective transformation of the position **p** in a Cartesian coordinate system and is defined by the zero-Doppler position X and the corresponding bistatic range R_b

$$X(\mathbf{p}) = \left\{ x : \frac{\partial R(x, \mathbf{p})}{\partial x} = 0 \right\}$$

$$R_b(\mathbf{p}) = R(X(\mathbf{p}), \mathbf{p})$$

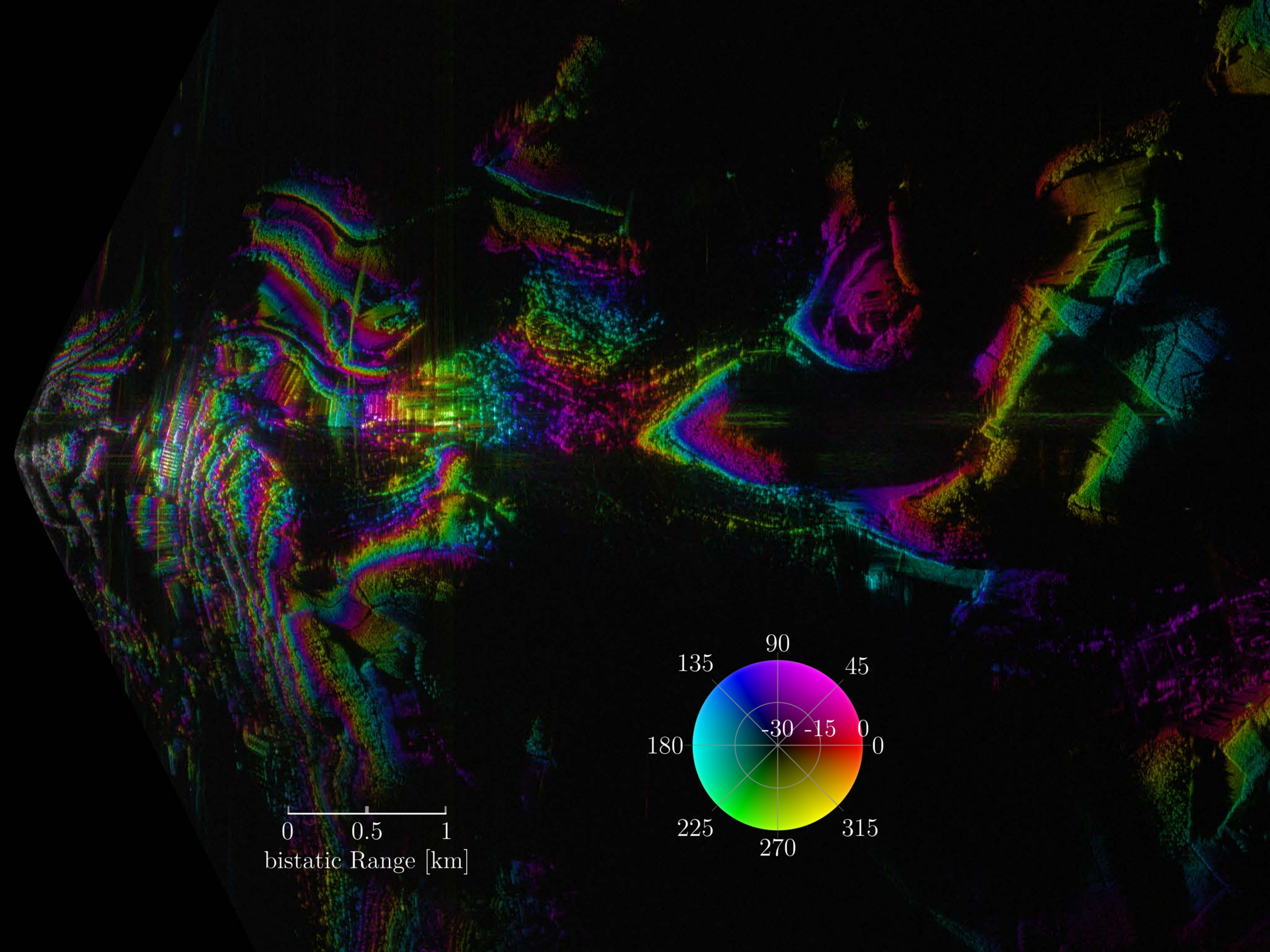

90
135
45
-30
-15
0
180
0
225
315
270
0
0.5
1
bistatic Range [km]

TerraSAR-X High Resolution Staring Spotlight Mode

A comparison of HS Mode / ST Mode

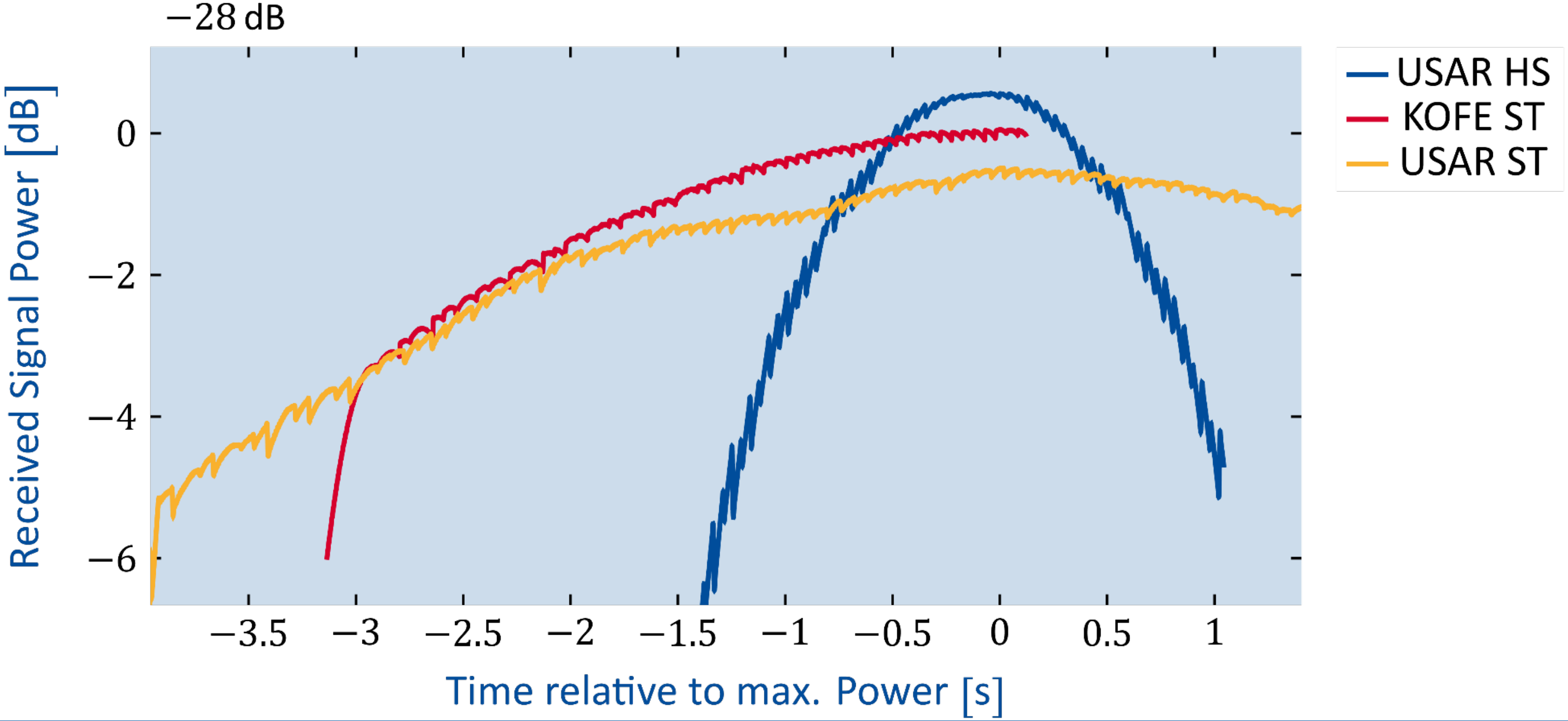

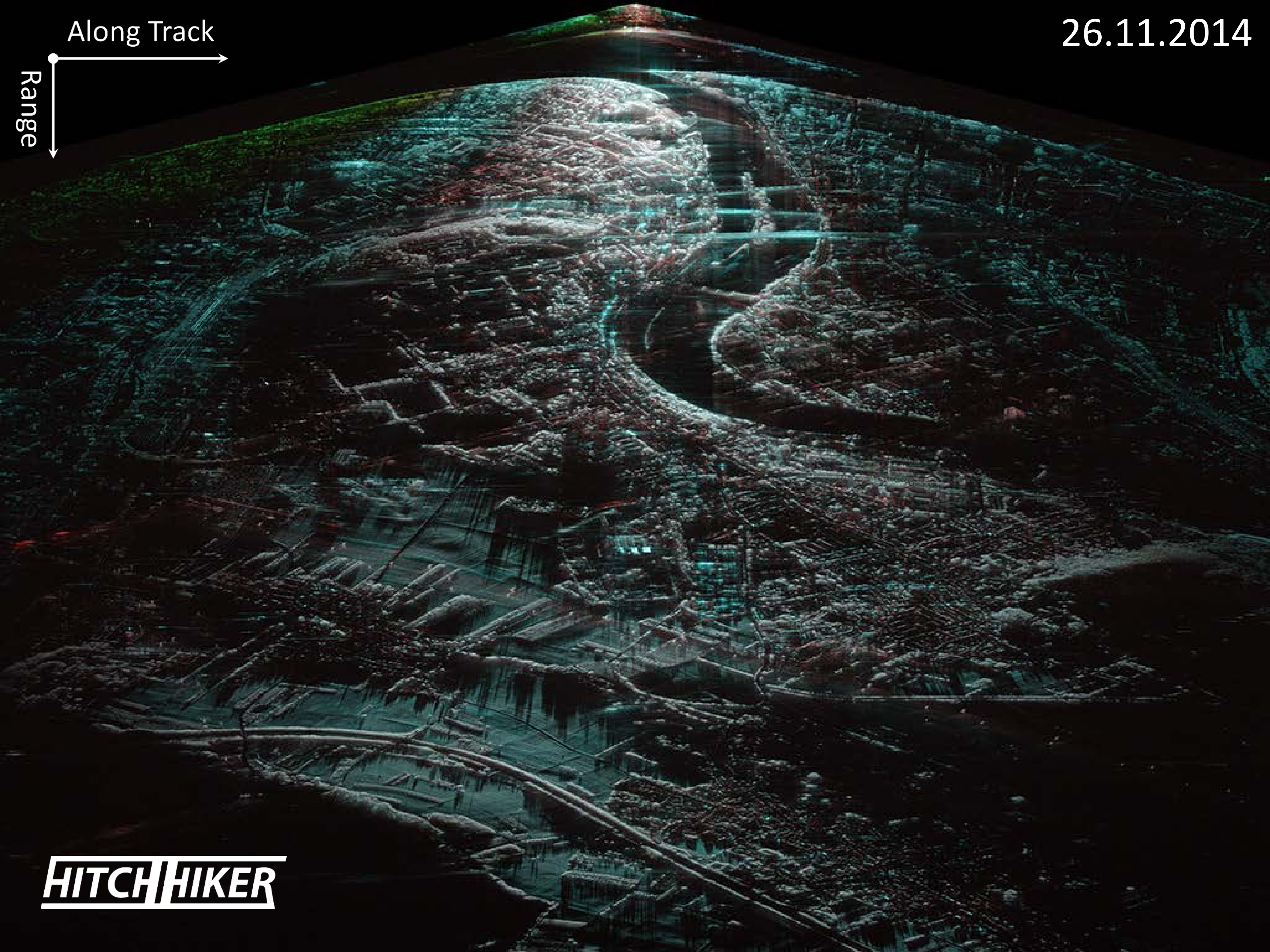
Along Track
Range
26.11.2014
HITCHHIKER

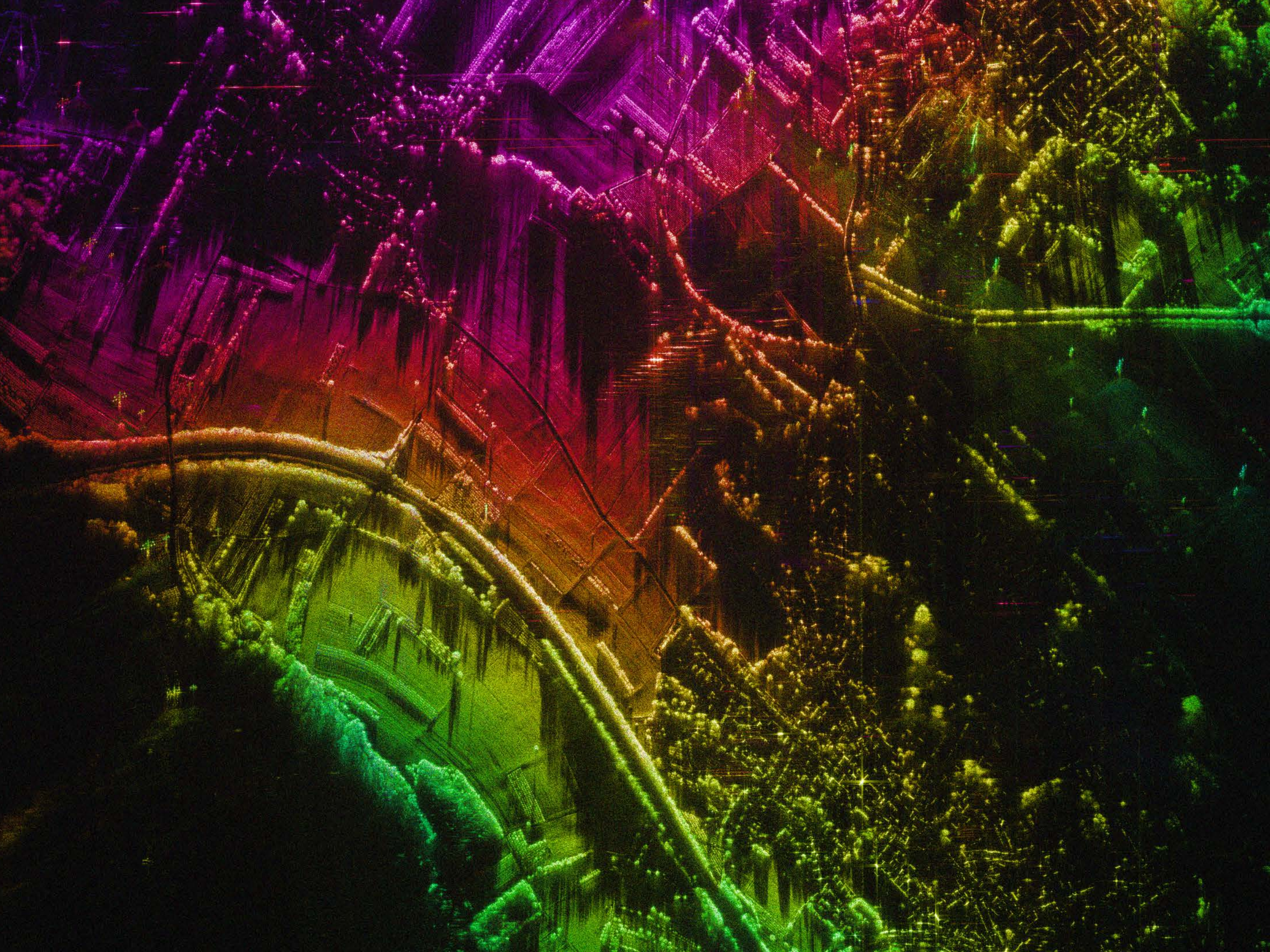

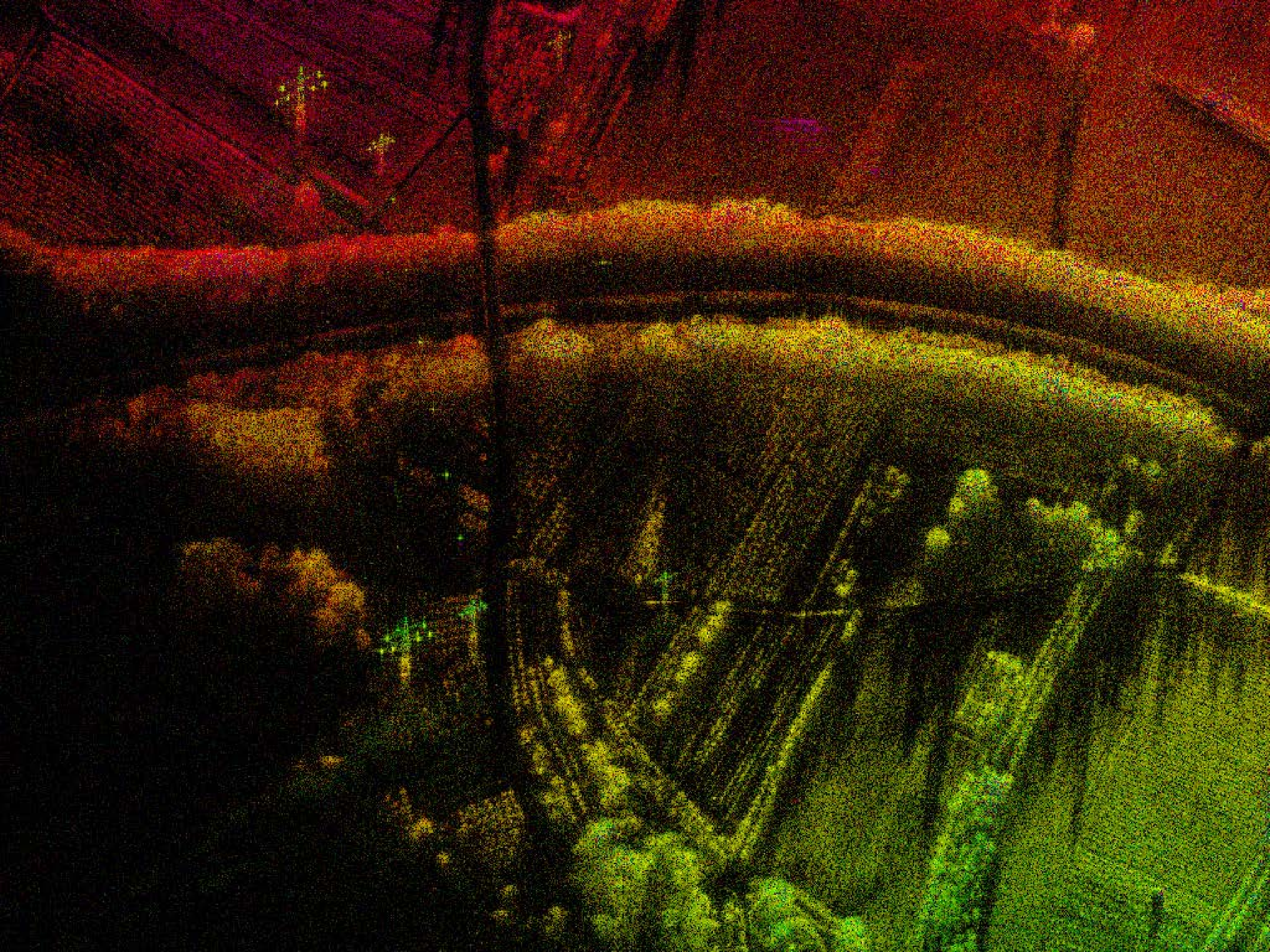

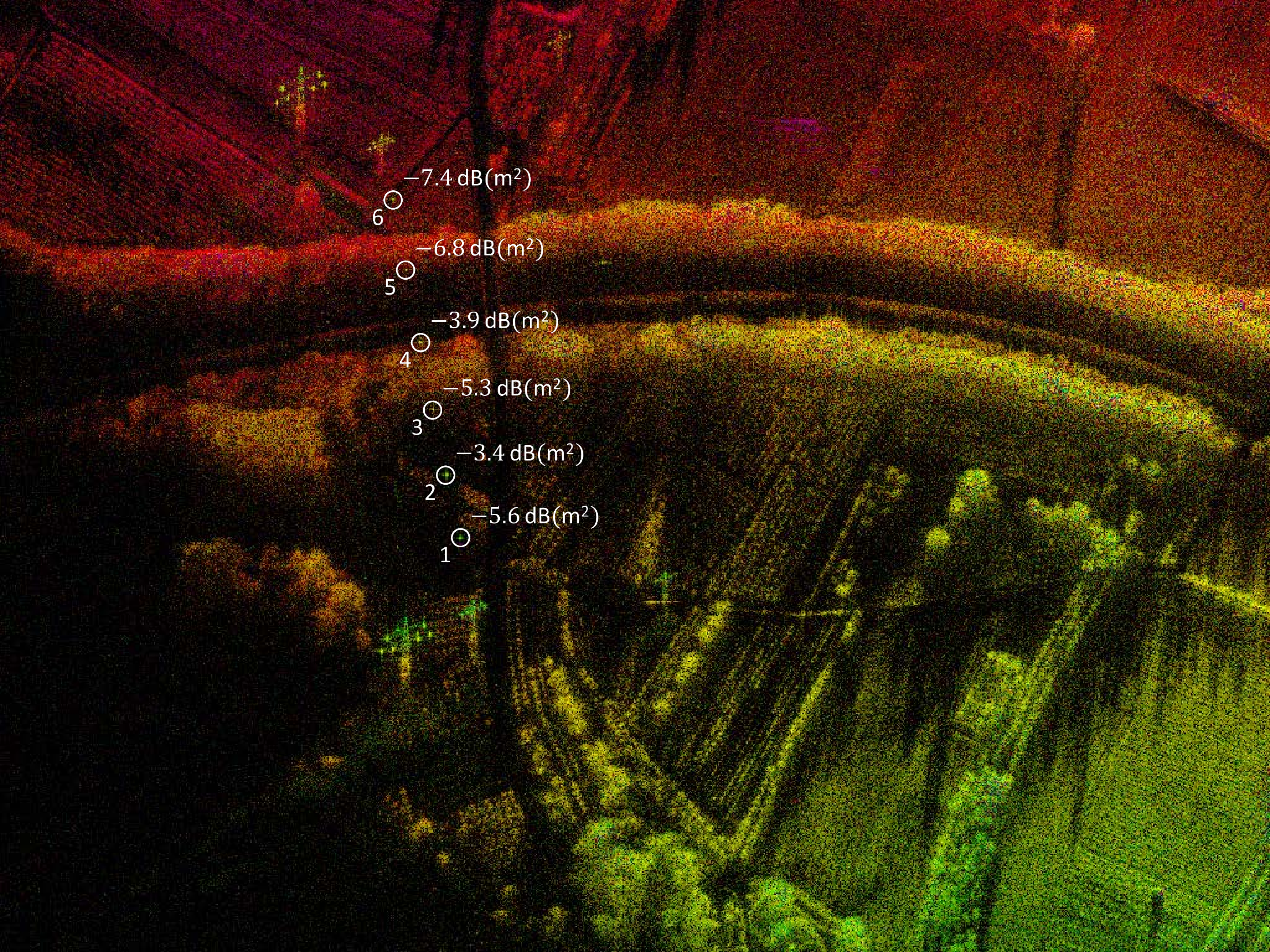

−7.4 dB(m²)
6
−6.8 dB(m²)
5
−3.9 dB(m²)
4
−5.3 dB(m²)
3
−3.4 dB(m²)
2
−5.6 dB(m²)
1

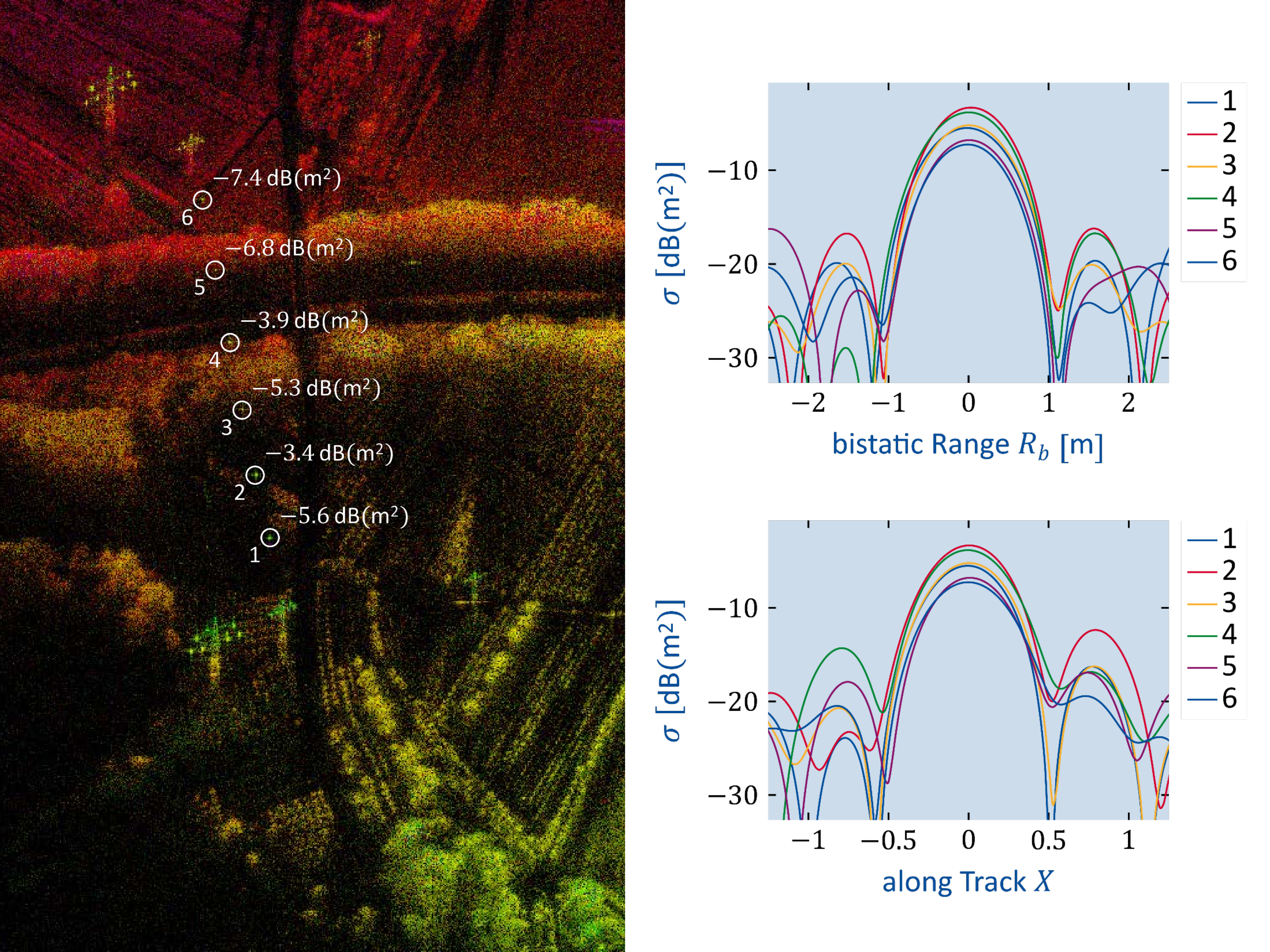

−7.4 dB(m²)
6
−6.8 dB(m²)
5
−3.9 dB(m²)
4
−5.3 dB(m²)
3
−3.4 dB(m²)
2
−5.6 dB(m²)
1
σ [dB(m²)]
−10
−20
−30
−2
−1
0
1
2
bistatic Range R_b [m]
1
2
3
4
5
6
σ [dB(m²)]
−10
−20
−30
−1
−0.5
0
0.5
1
along Track X
1
2
3
4
5
6

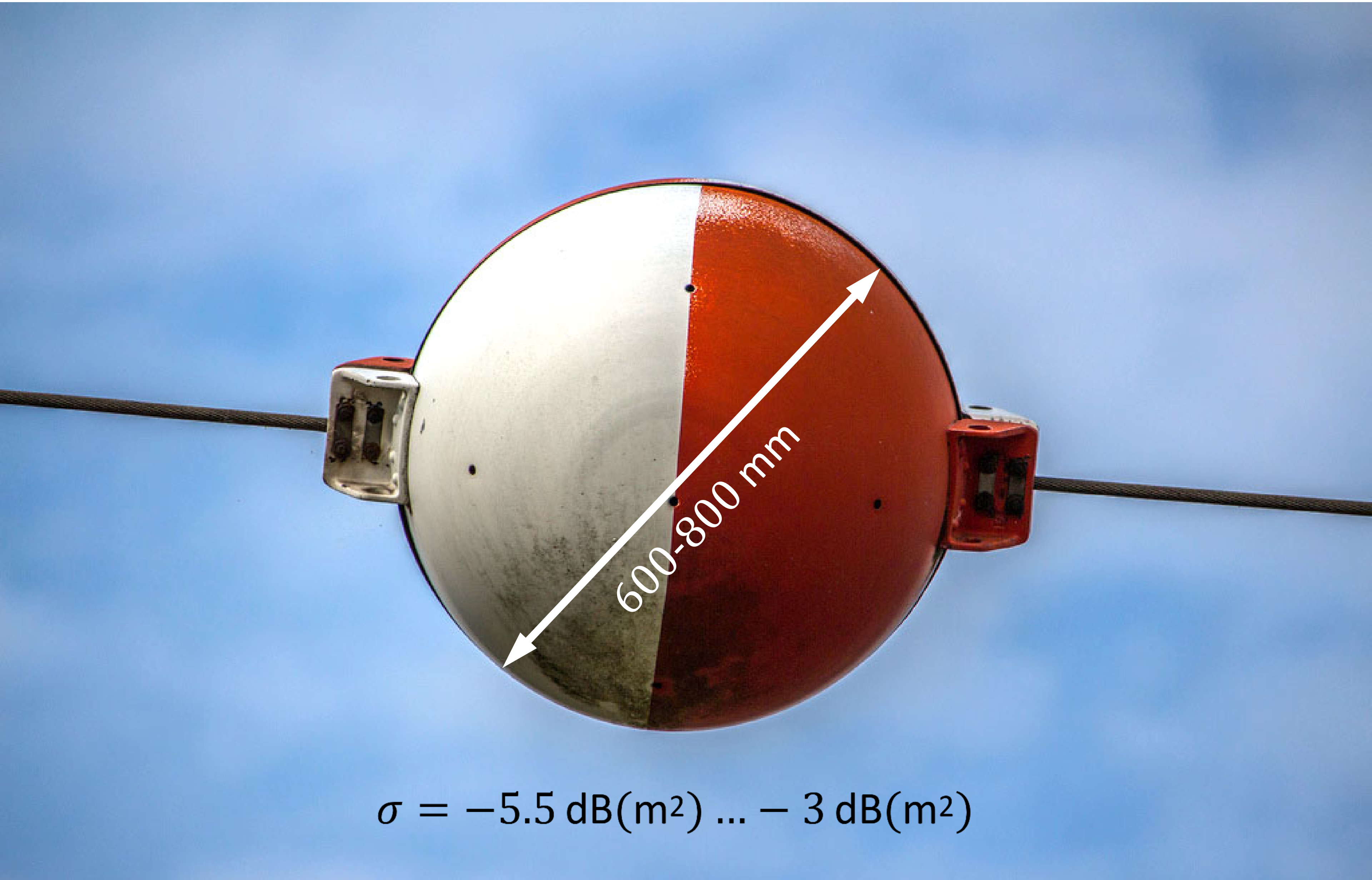

$\sigma = -5.5\,\mathrm{dB(m^2)} \ldots -3\,\mathrm{dB(m^2)}$

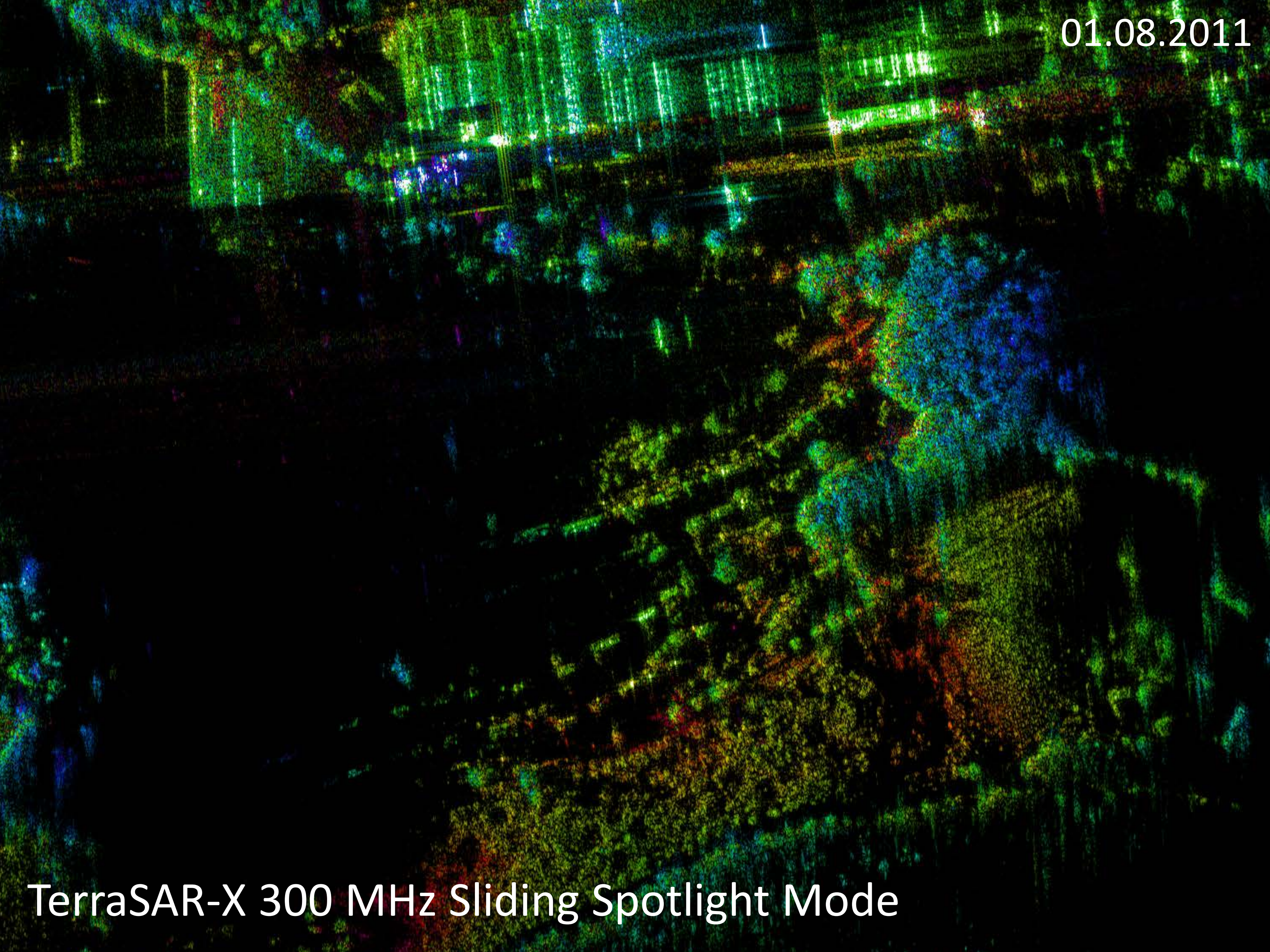
01.08.2011
TerraSAR-X 300 MHz Sliding Spotlight Mode

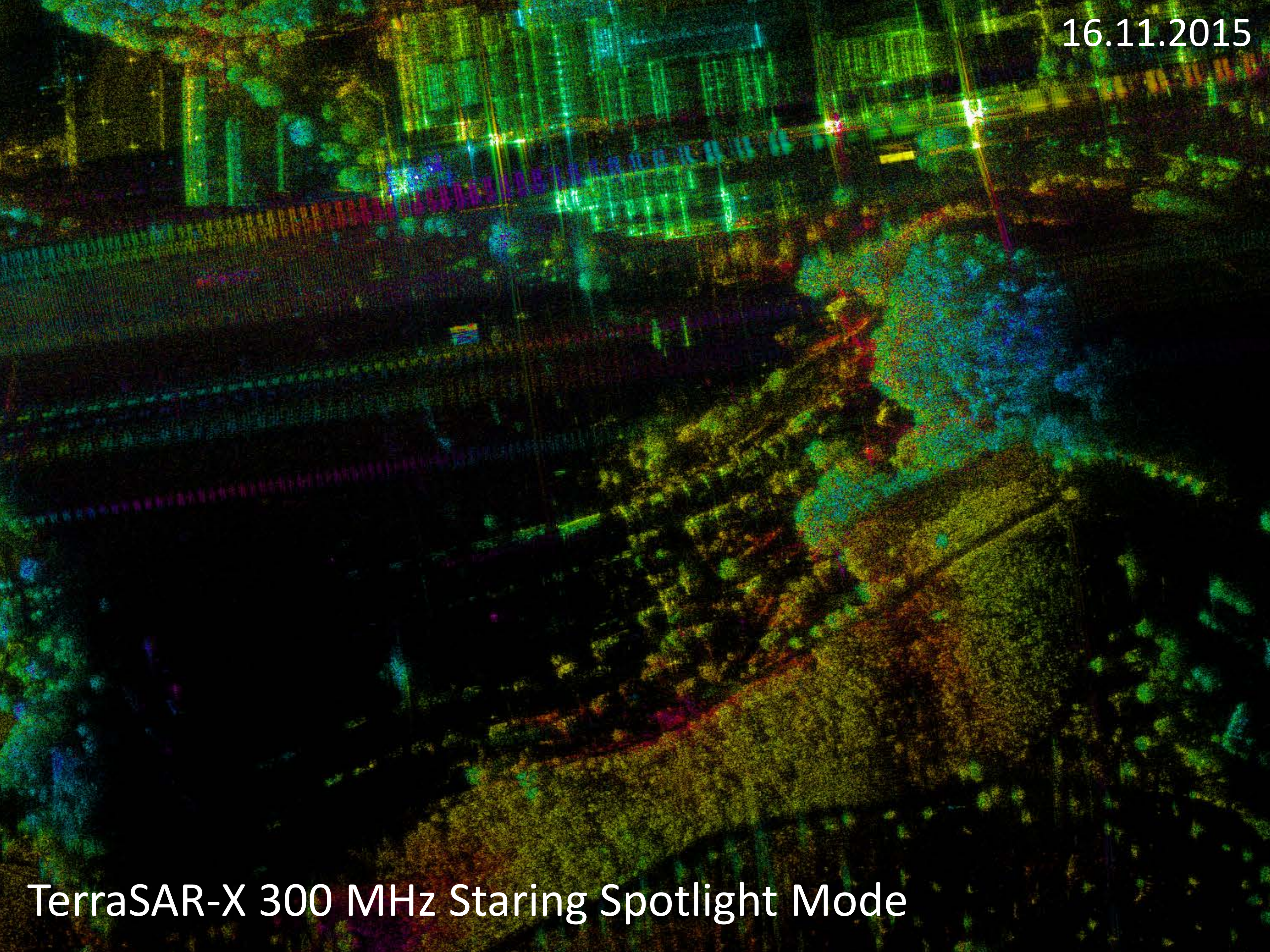
16.11.2015
TerraSAR-X 300 MHz Staring Spotlight Mode

High Resolution Bistatic SAR Tomograhy Experiment

Fraunhofer FHR

Bandwidth	1.8 GHz@9.45 GHz
Pulse Length	5.08 μs
PRF	2 kHz
Mode	Sliding Spotlight

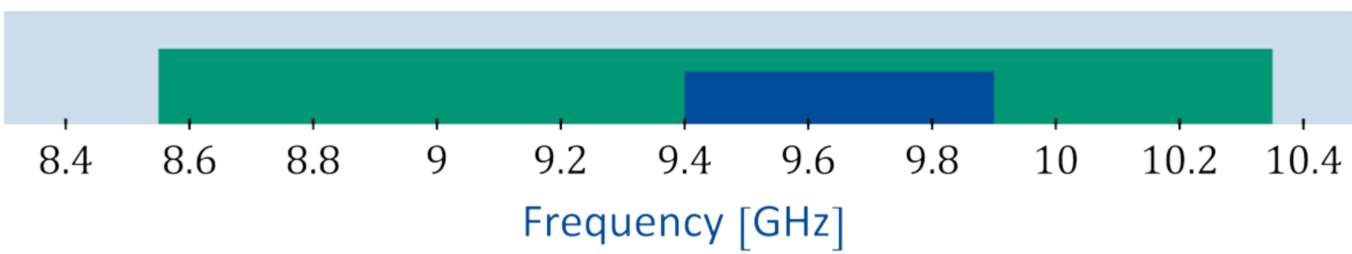

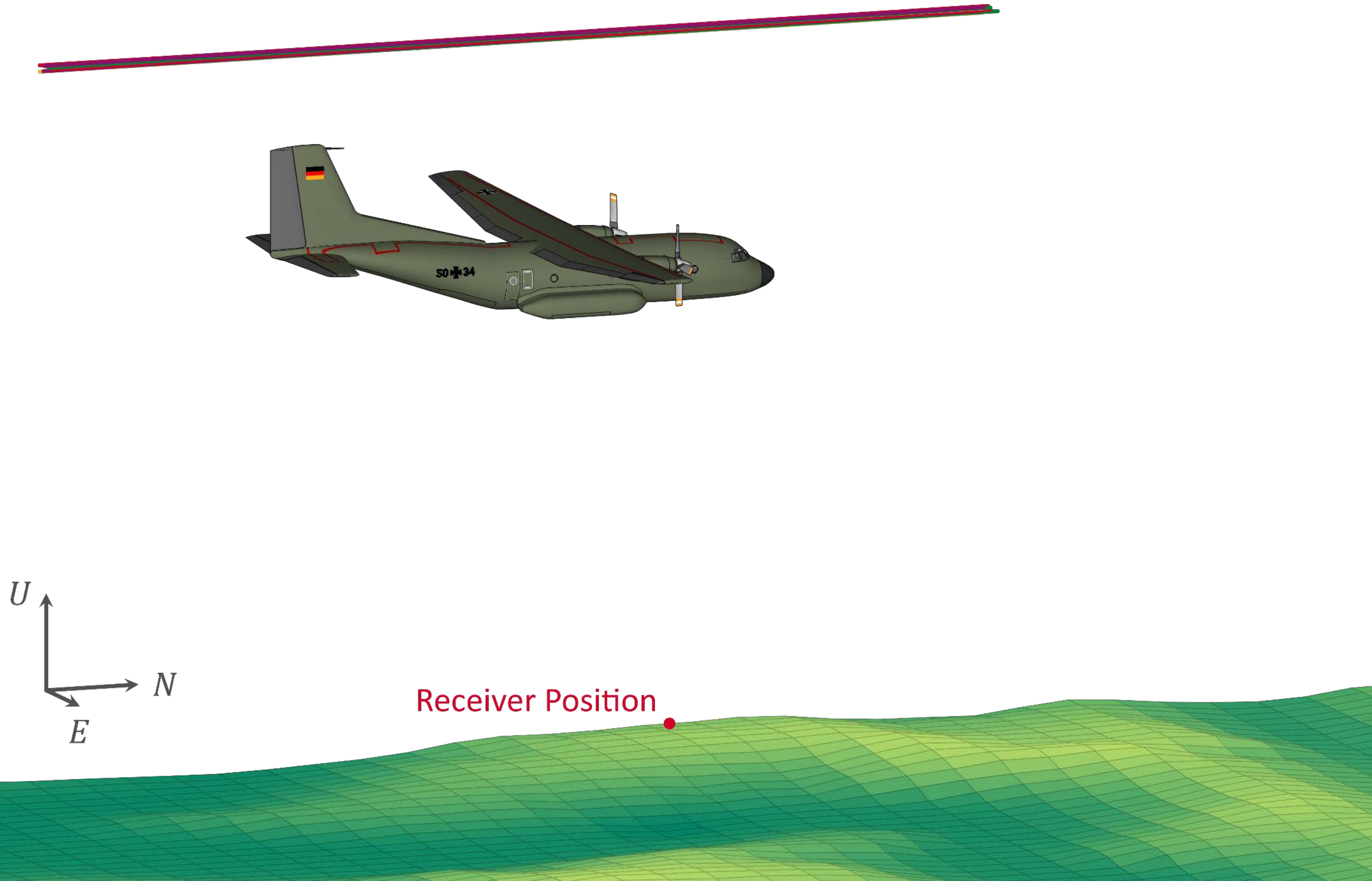

U
N
E
Receiver Position

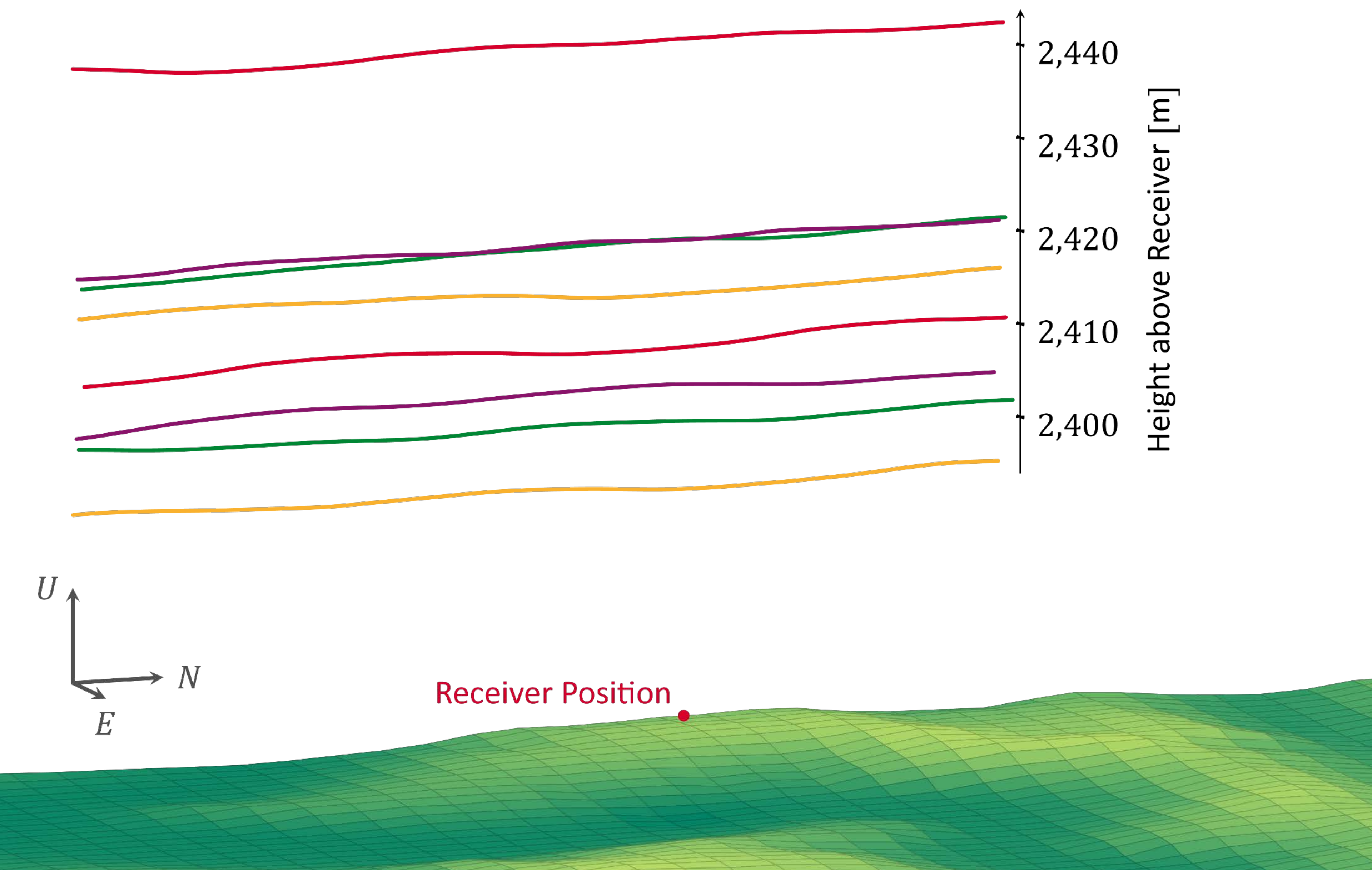
2,440
2,430
2,420
2,410
2,400
Height above Receiver [m]
U
N
E
Receiver Position

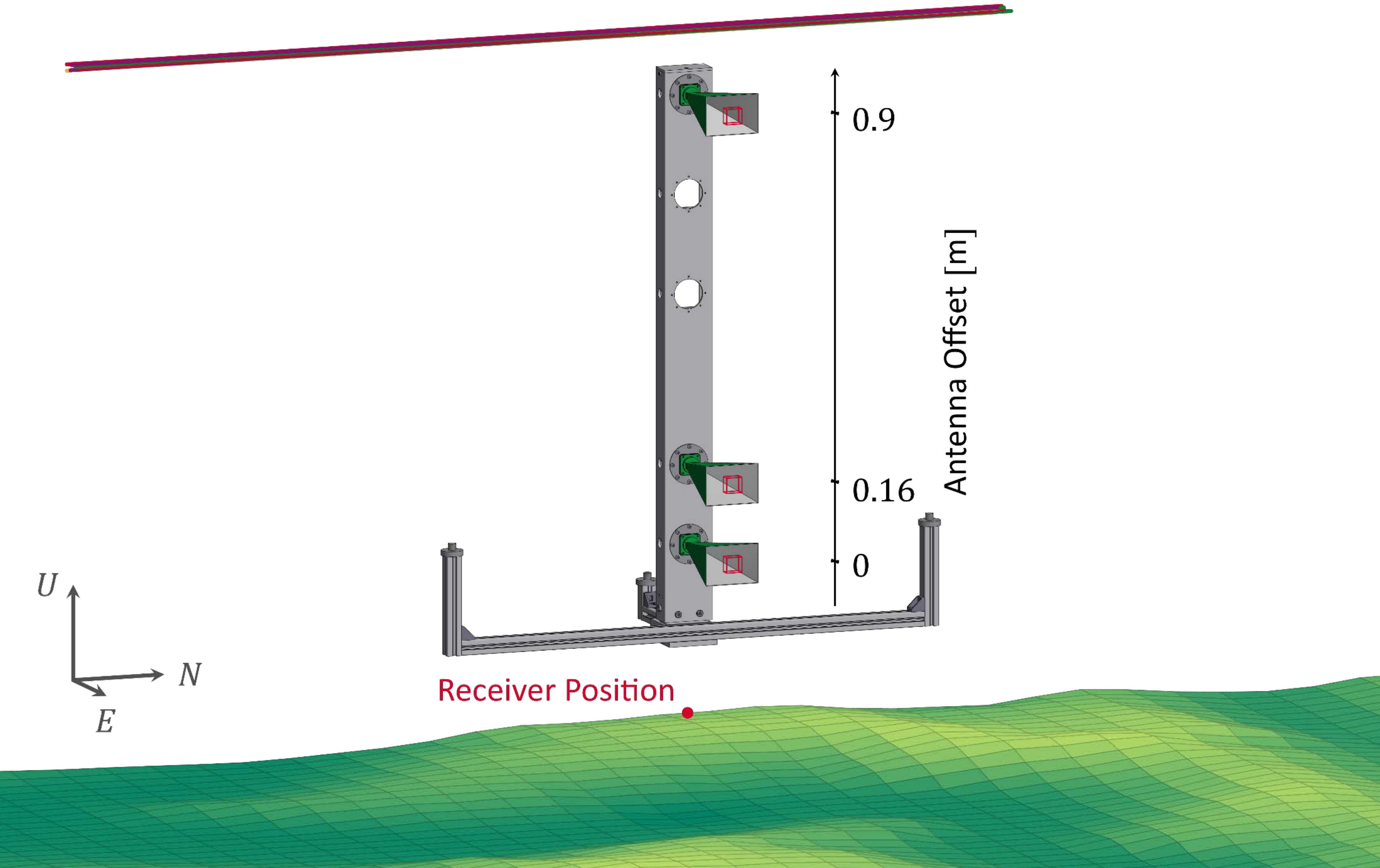

0.9
0.16
0
Antenna Offset [m]
U
N
E
Receiver Position

Tomo SAR Signal Model

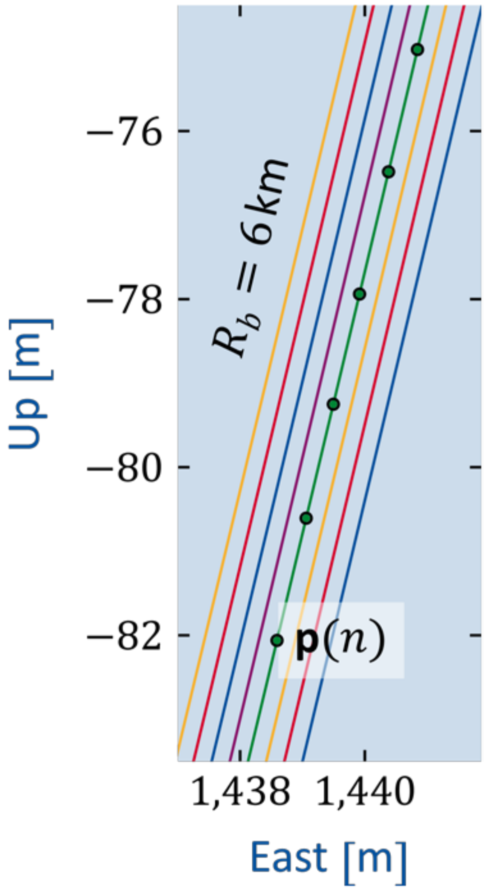

Tomo SAR Signal Model

$$\mathbf{y} = \mathbf{A} \cdot \mathbf{x}$$

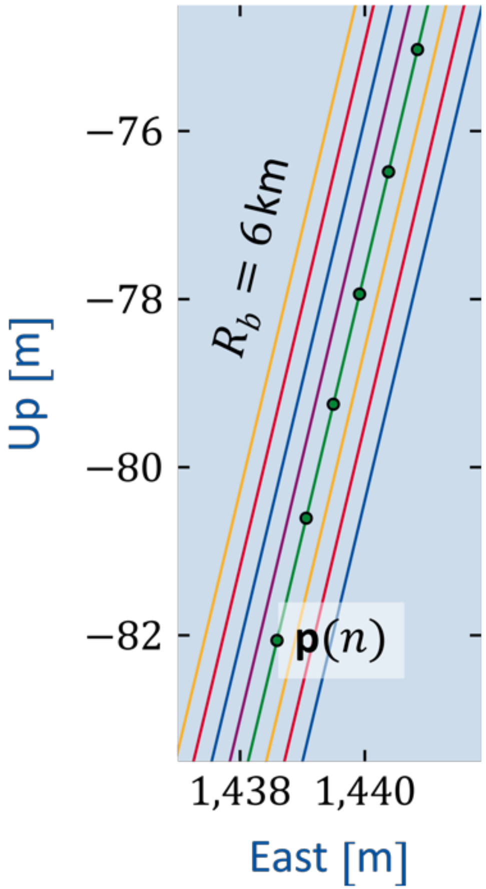

Tomo SAR Signal Model

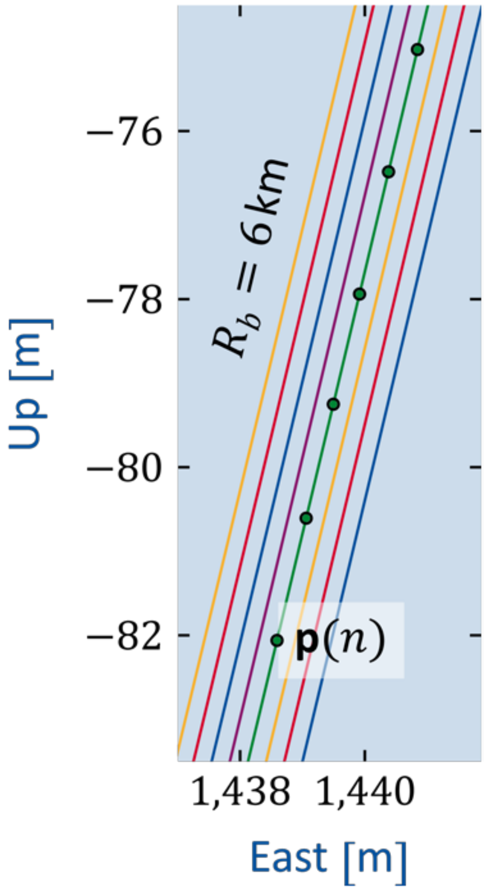

$$\mathbf{y} = \mathbf{A} \cdot \mathbf{x}$$

$$\mathbf{x} = (x_n) \in \mathbb{C}^N$$

Tomo SAR Signal Model

$$\mathbf{y} = \mathbf{A} \cdot \mathbf{x}$$

$$\mathbf{x} = (x_n) \in \mathbb{C}^N$$

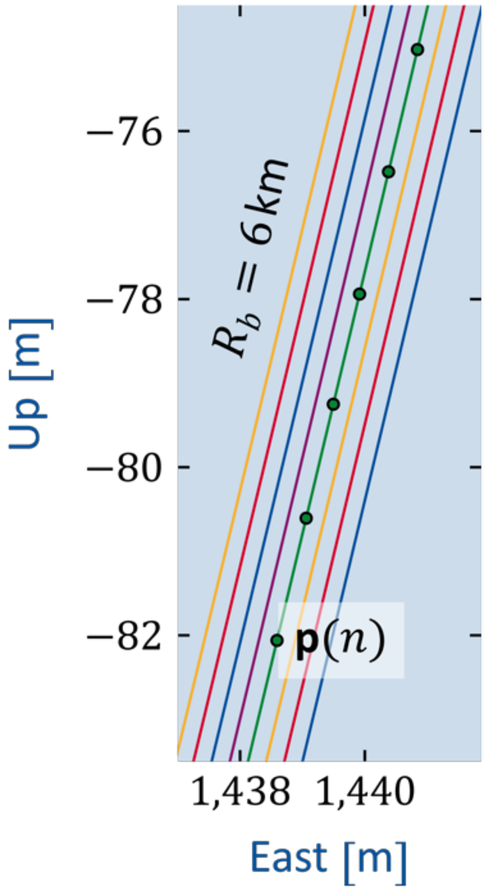

$$R(x,m,n) = \|\mathbf{p}_t(x,m) - \mathbf{p}(n)\|_2 + \|\mathbf{p}_r(m) - \mathbf{p}(n)\|_2$$

$$X(m,n) = \left\{x : \frac{\partial R(x,m,n)}{\partial x} = 0\right\}$$

$$R_b(m,n) = R\big(X(m,n), m, n\big)$$

Tomo SAR Signal Model

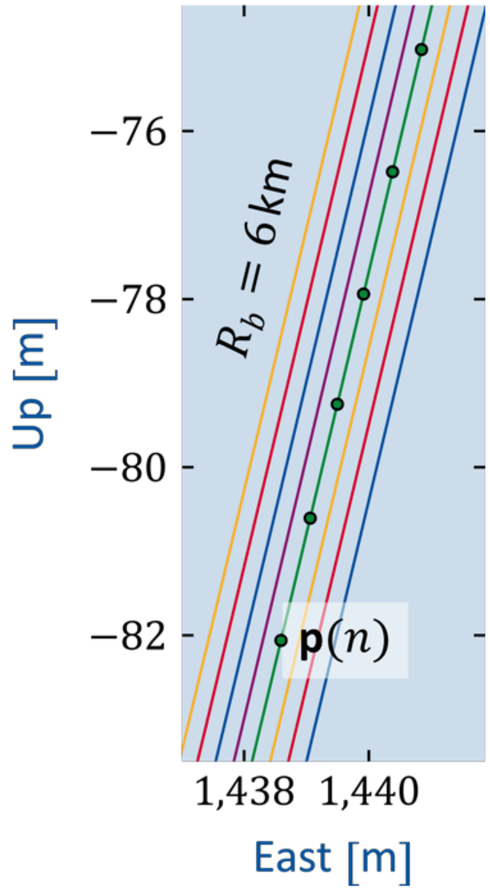

$$\mathbf{y} = \mathbf{A} \cdot \mathbf{x}$$

$$\mathbf{x} = (x_n) \in \mathbb{C}^N$$

$$R(x,m,n) = \|\mathbf{p}_t(x,m) - \mathbf{p}(n)\|_2 + \|\mathbf{p}_r(m) - \mathbf{p}(n)\|_2$$

$$X(m,n) = \left\{ x : \frac{\partial R(x,m,n)}{\partial x} = 0 \right\}$$

$$R_b(m,n) = R\big(X(m,n), m, n\big)$$

$$\mathbf{A} = (a_{mn}) \in \mathbb{C}^{M \times N}$$

$$a_{mn} = \exp\big(-jk_0 R_b(m,n)\big)$$

Tomo SAR Signal Model

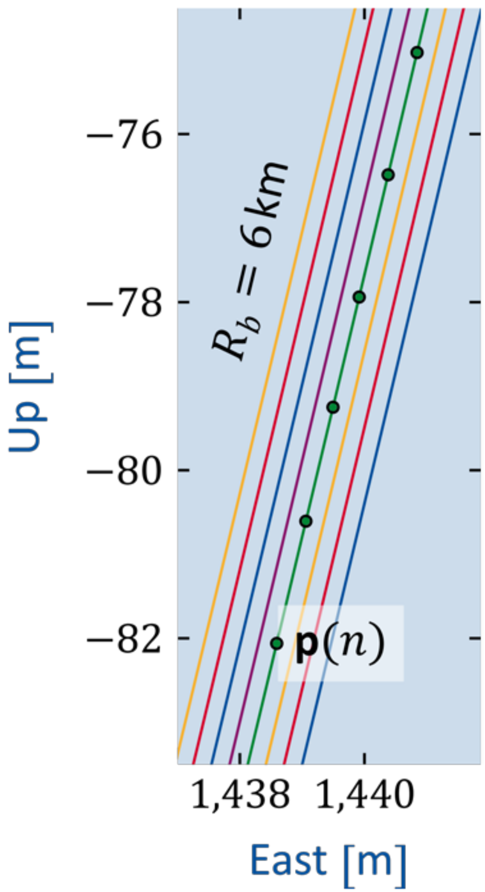

$$\mathbf{y} = \mathbf{A} \cdot \mathbf{x}$$

$$\mathbf{x} = (x_n) \in \mathbb{C}^N$$

$$R(x,m,n) = \|\mathbf{p}_t(x,m) - \mathbf{p}(n)\|_2 + \|\mathbf{p}_r(m) - \mathbf{p}(n)\|_2$$

$$X(m,n) = \left\{ x : \frac{\partial R(x,m,n)}{\partial x} = 0 \right\}$$

$$R_b(m,n) = R\big(X(m,n),m,n\big)$$

$$\mathbf{A} = (a_{mn}) \in \mathbb{C}^{M \times N}$$

$$a_{mn} = \exp\big(-jk_0 R_b(m,n)\big)$$

$$\mathbf{y} = (y_m) \in \mathbb{C}^M$$

$$y_m = I_m\big(R_b(m,\cancel{n}), X(m,\cancel{n})\big)$$

Some definitions

Coherence of the sensing matrix:

$$\mu(A) =: \max_{1\le i\ne j\le N} \frac{\left|\left\langle \underline{a}_i, \underline{a}_j \right\rangle\right|}{\left\|\underline{a}_i\right\|_2 \cdot \left\|\underline{a}_j\right\|_2} = \max_{1\le i\ne j\le N} \frac{1}{M}\left|\left\langle \underline{a}_i, \underline{a}_j \right\rangle\right|$$

Letting:

$$\Phi = \frac{1}{M} A^H A = \frac{1}{M}\begin{bmatrix} \langle \underline{a}_1, \underline{a}_1 \rangle & \langle \underline{a}_1, \underline{a}_2 \rangle & & \langle \underline{a}_1, \underline{a}_N \rangle \\ \langle \underline{a}_2, \underline{a}_1 \rangle & \langle \underline{a}_2, \underline{a}_2 \rangle & & \langle \underline{a}_2, \underline{a}_N \rangle \\ & & & \\ \langle \underline{a}_N, \underline{a}_1 \rangle & & & \langle \underline{a}_N, \underline{a}_N \rangle \end{bmatrix} = \left[\Phi_{i,j}\right]$$

Matched filter result

We have: $\Phi_{ii} = 1$ and $\Phi_{ij} = \frac{1}{M}\left\langle \underline{a}_i, \underline{a}_j \right\rangle$ *and* $\mu(A) = \max_{1\le i\ne j\le N} \left|\Phi_{ij}\right|$

Plot of one row of: $\Phi_{\text{row } n_0} = \left[\frac{1}{M} A^H A\right]_{\text{row } n_0} = \left[\Phi_{n_0, j}\right]_{1 \le j \le N}$

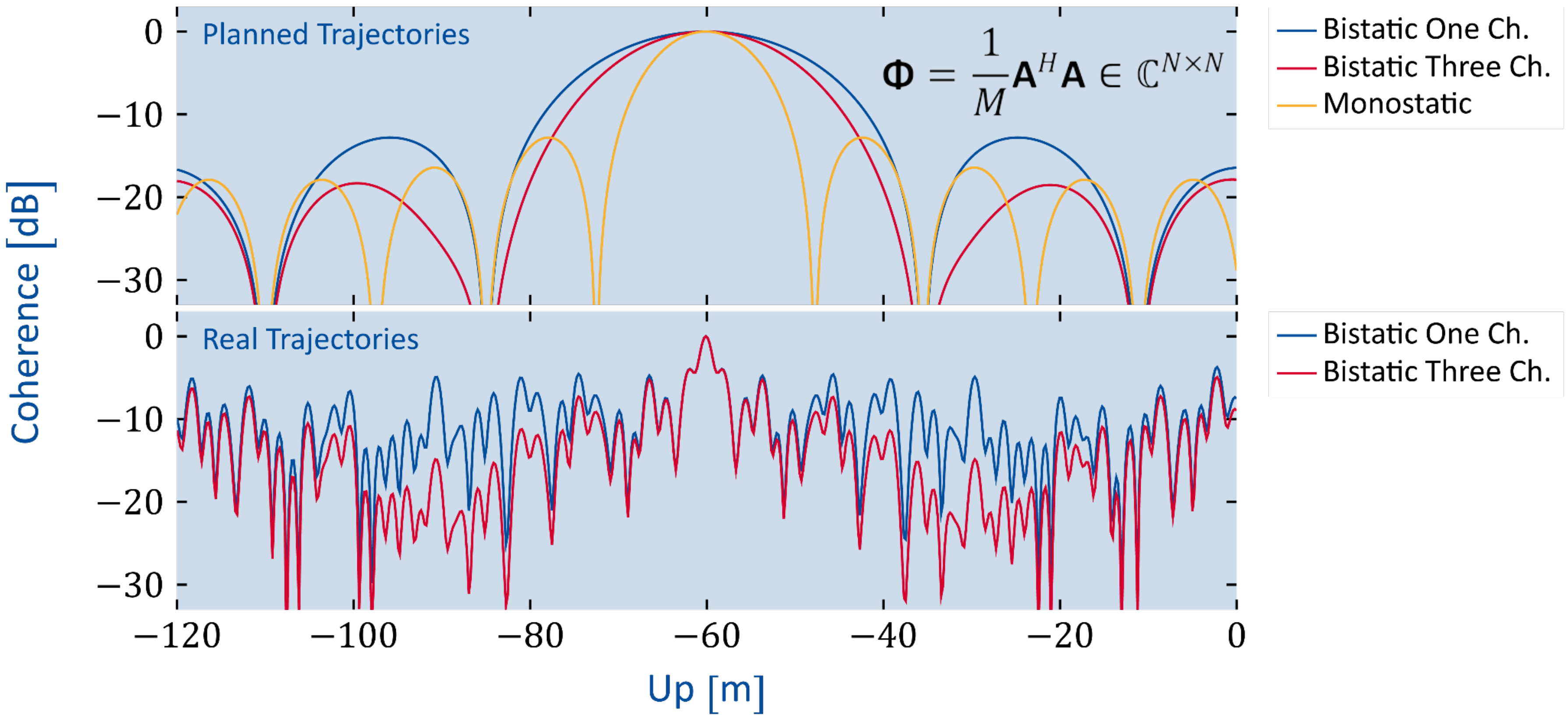

ℓ_1- Regularized Least Squares

$$\hat{\mathbf{x}} = \arg\min_{\mathbf{x}} \left\{ \|\mathbf{x}\|_1 + \frac{\gamma}{2} \|\mathbf{A}\mathbf{x} - \mathbf{y}\|_2^2 \right\}$$

[1] X. X. Zhu and R. Bamler (2012, Jan.). Super-Resolution Power and Robustness of Compressive Sensing for Spectral Estimation With Application to Spaceborne Tomographic SAR. *IEEE Transactions on Geoscience and Remote Sensing*, vol. 50, no. 1, pp.247-258.

[2] S. Foucart and H. Rauhut, ”Chambolle and Pock’s Primal-Dual Algorithm”, in *A Mathematical Introduction to Compressive Sensing*, Springer New York, 2013, pp. 486-487.

Radar processing using geostationary satellites

- Permanent availability
- Cost effective
- Large coverage
- Different Applications
  - Imaging
  - Change detection
  - Tracking

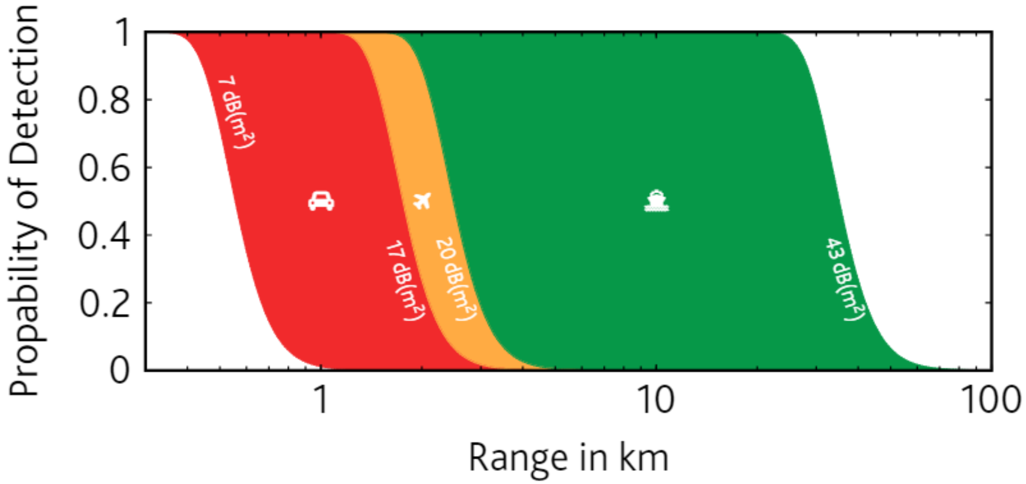

Astra Satellite System

- Geostationary Orbit
- Co-located Satellites
- Television and Radio Broadcasting

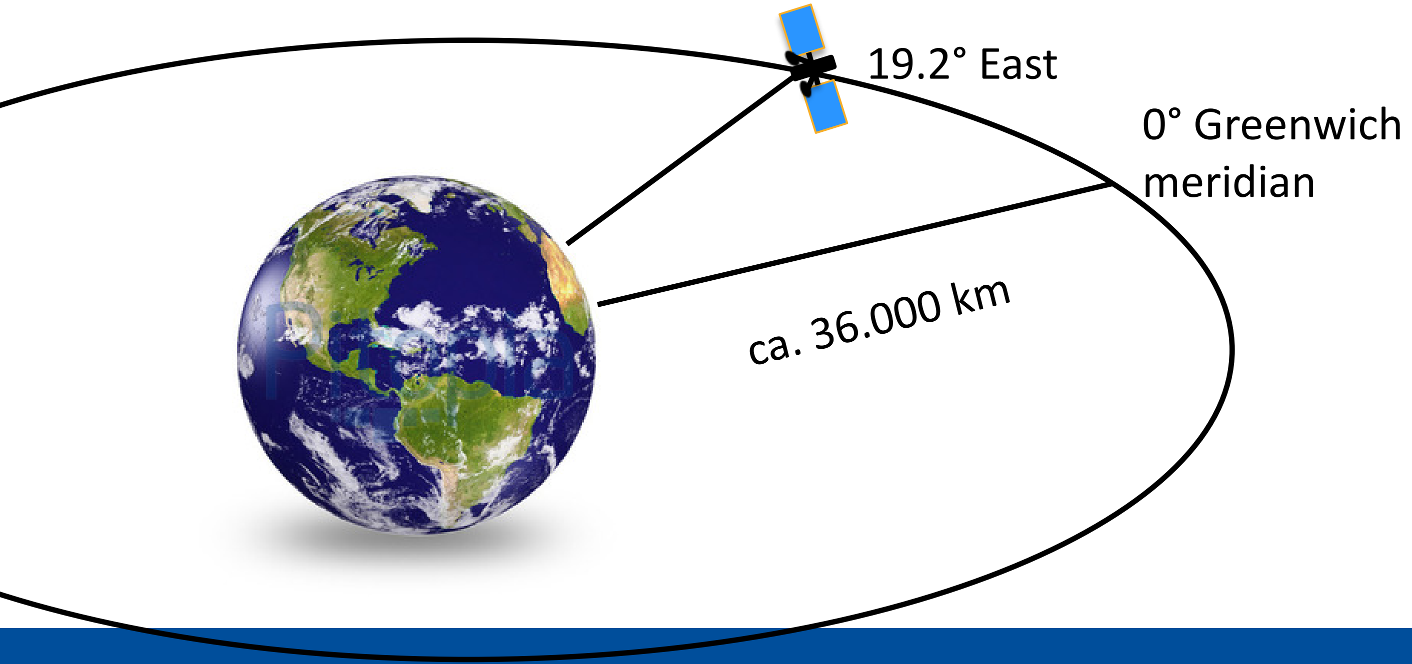

Astra Satellite System

- Geostationary Orbit
- Co-located Satellites
- Television and Radio Broadcasting

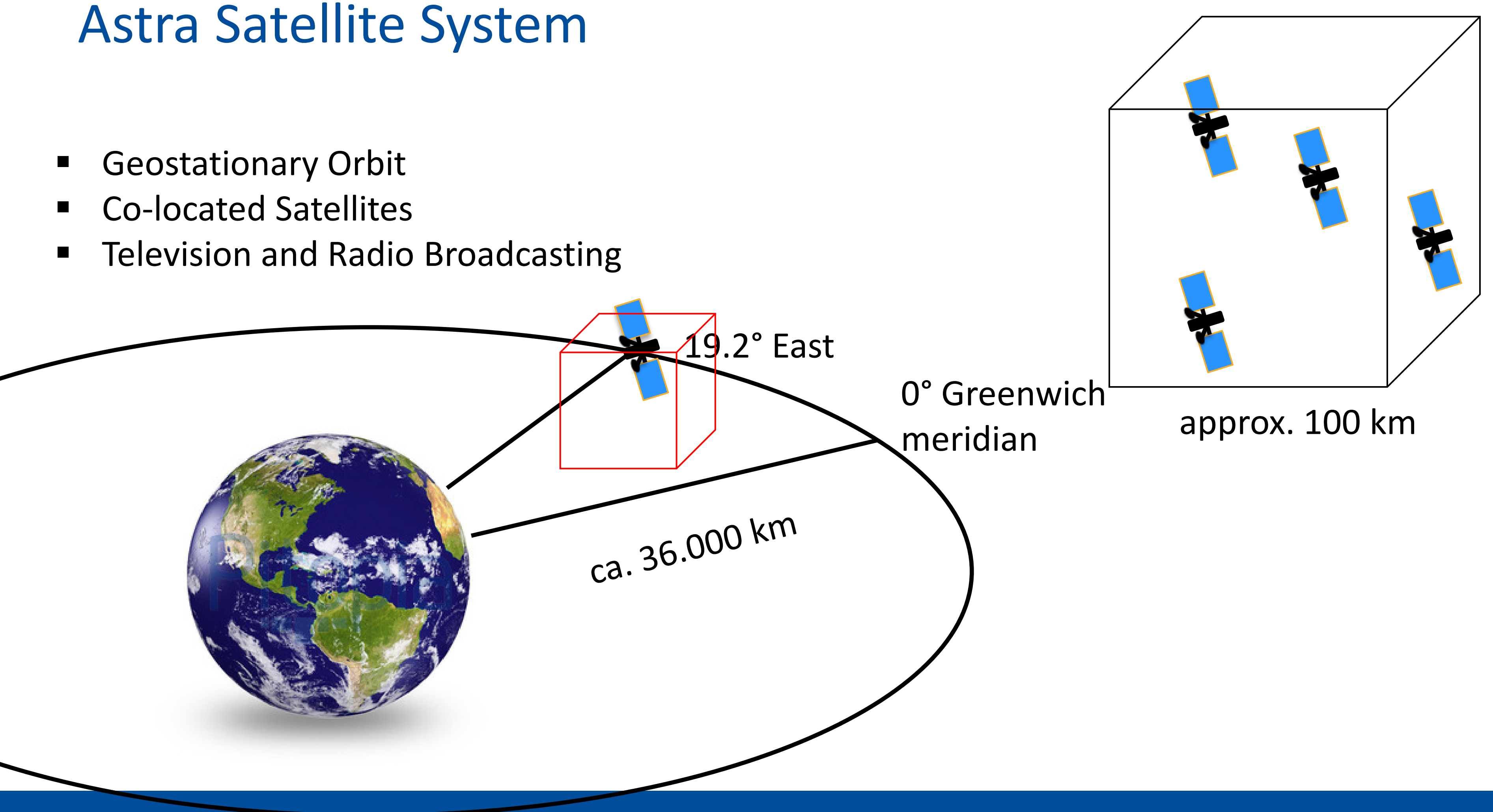

Astra Satellite System

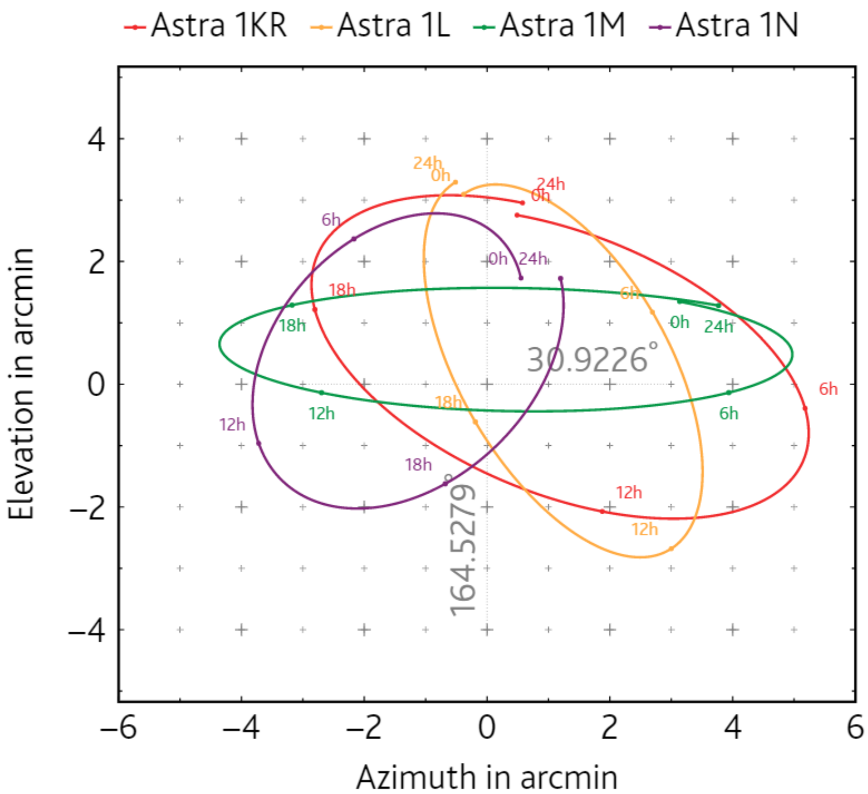

- Ku-Band 10.7 GHz – 12.75 GHz
- Transponders distributed on different Satellites

- Cross Range Resolution (SAR): 13 m
- Range Resolution:
  - Full Bandwidth (2.05 GHz): 15 cm
  - 1 Transponder (30 MHz): 10 m

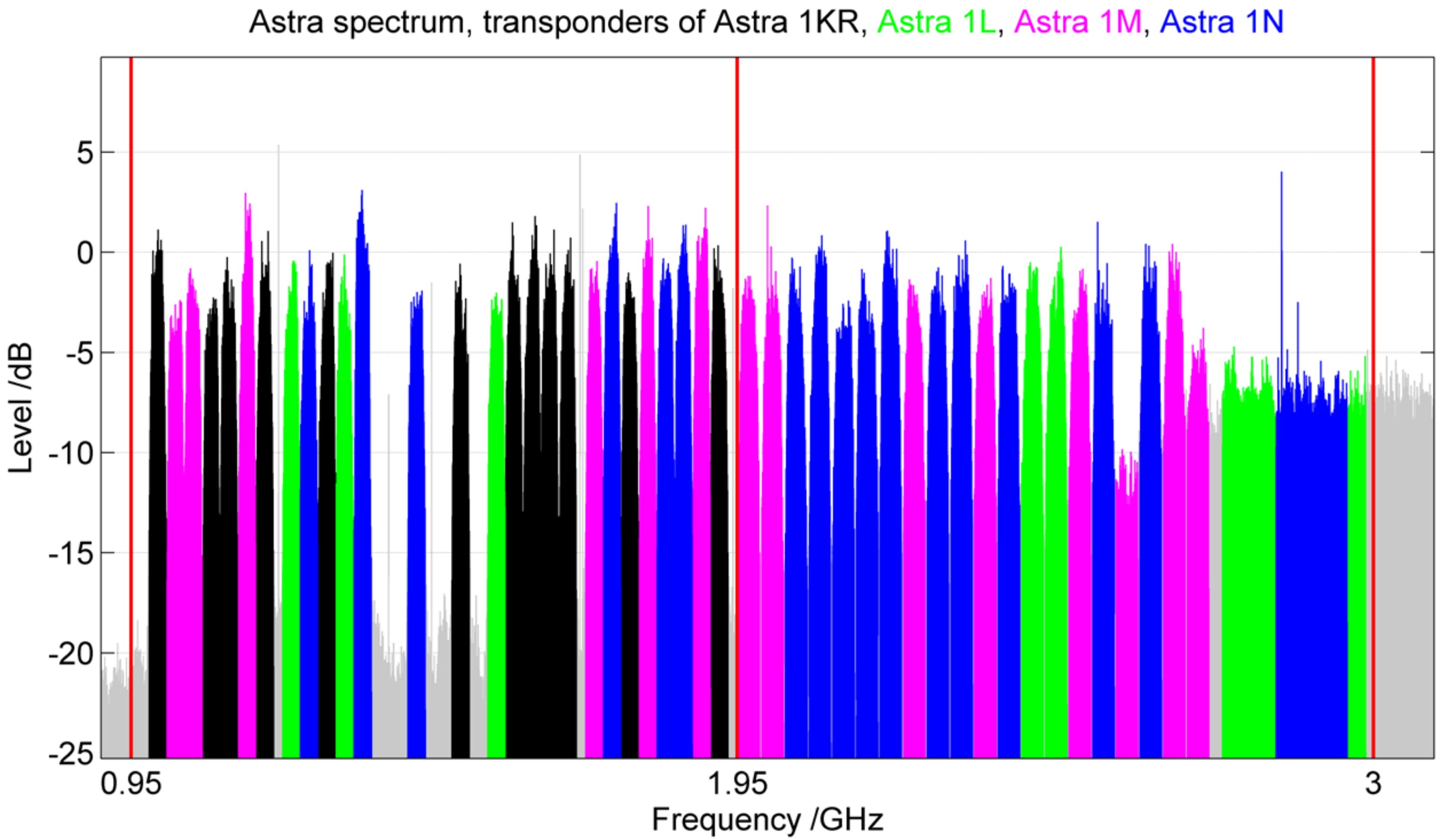
Astra spectrum, transponders of Astra 1KR, Astra 1L, Astra 1M, Astra 1N
Level /dB
5
0
-5
-10
-15
-20
-25
0.95
1.95
3
Frequency /GHz

SAR Imaging Experiment

- Recording System: HITCHHIKER
- Location: ZESS, University of Siegen
- Received Signal: Astra 19.2° East, low Band, horizontal Polarization
- Sampling Rate: 8 GS/s
- Record Length per Pulse: 6.25 ms
- Pulse Repetition Interval: 20 s
- Integration Time: up to 12 h

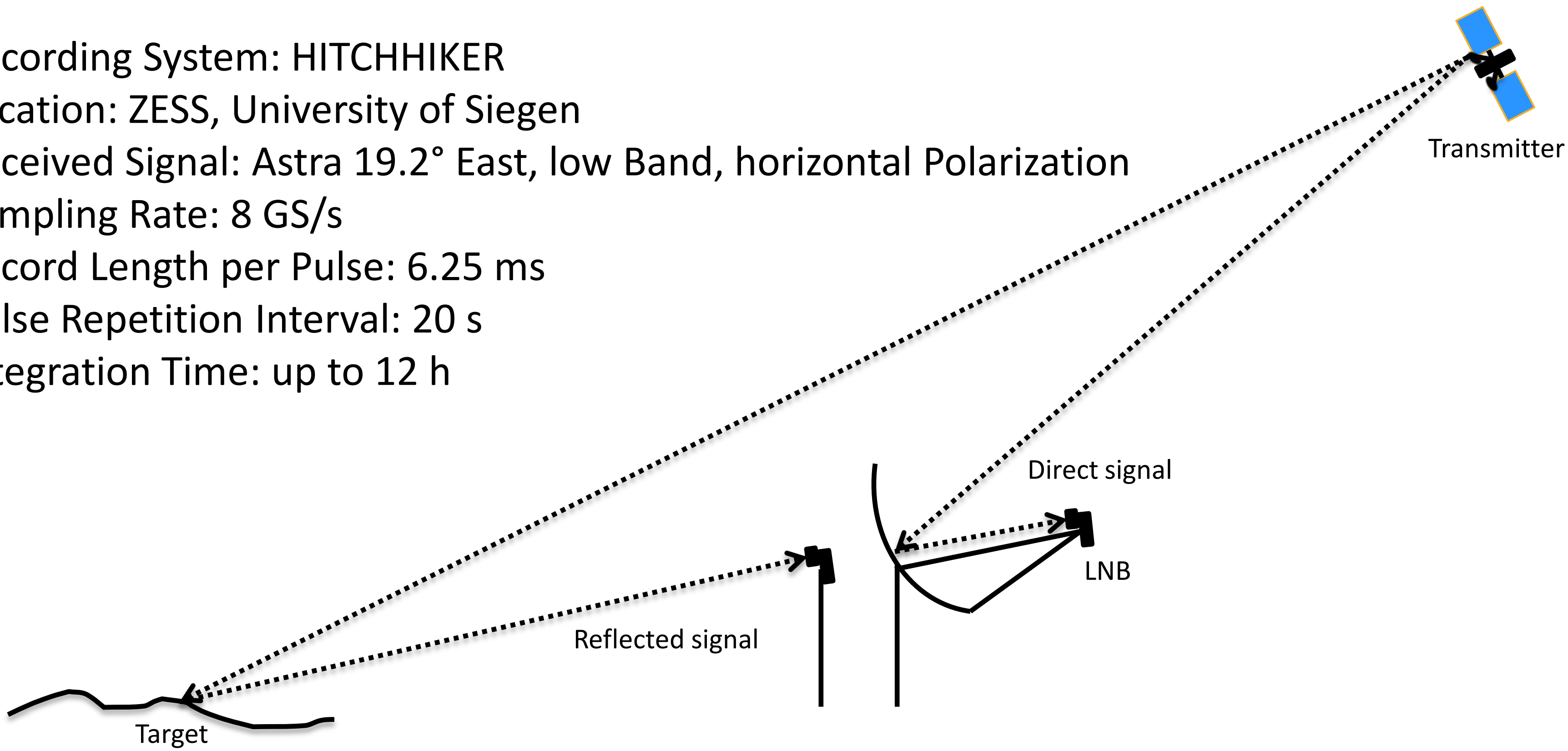

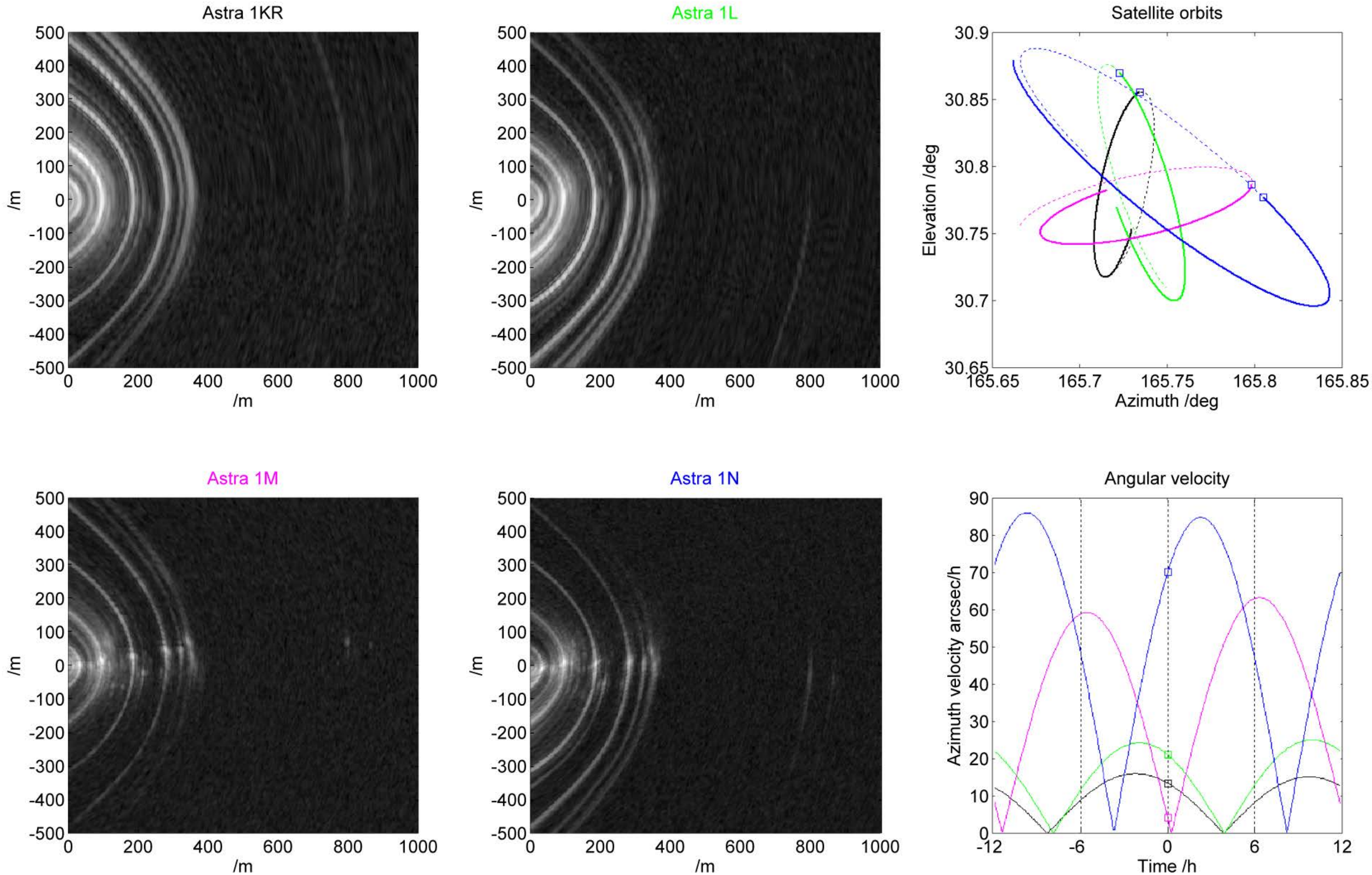
Astra 1KR
Astra 1L
Satellite orbits
Astra 1M
Astra 1N
Angular velocity
/m
Elevation /deg
Azimuth /deg
Azimuth velocity arcsec/h
Time /h

Passive Radar System

- Dedicated DVB-S passive radar
- Radar applications
  - Moving target detection/Tracking
  - Moving receiver platform
  - ISAR imaging
  - Modular multistatic system

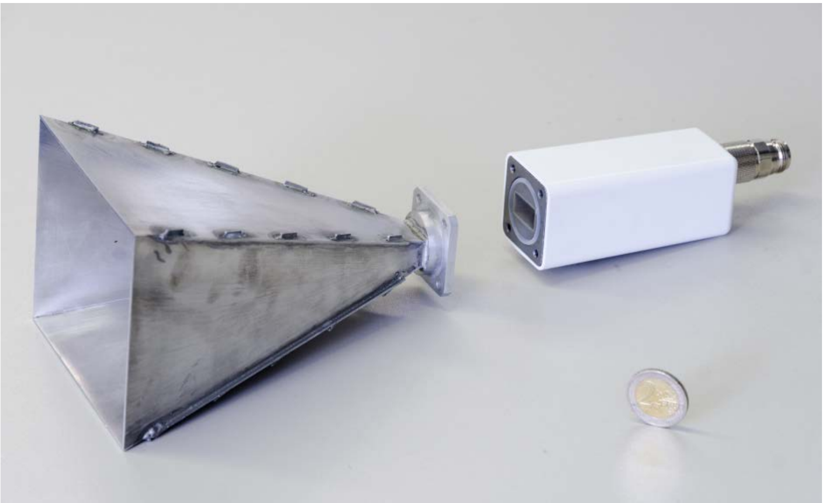

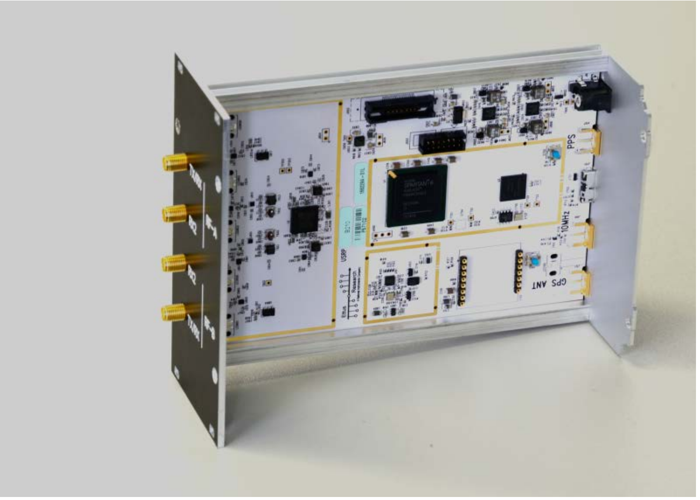

Passive Radar System

- Dedicated DVB-S passive radar
- Radar applications
  - Moving target detection/Tracking
  - Moving receiver platform
  - ISAR imaging
  - Modular multistatic system

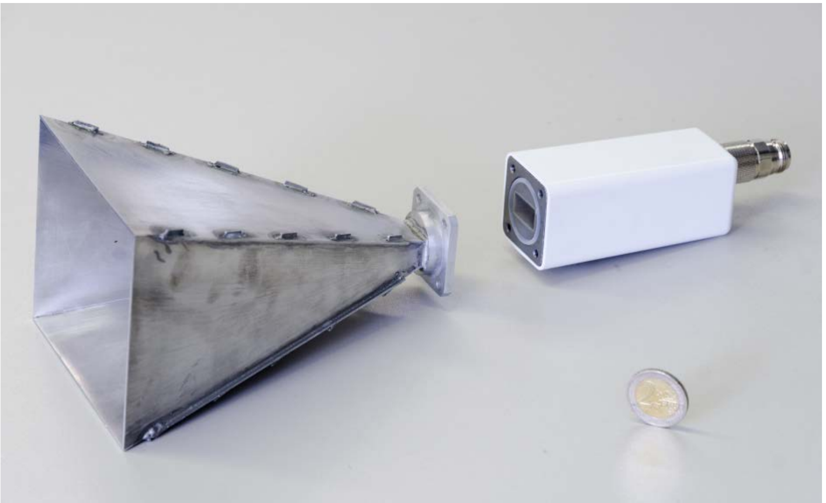

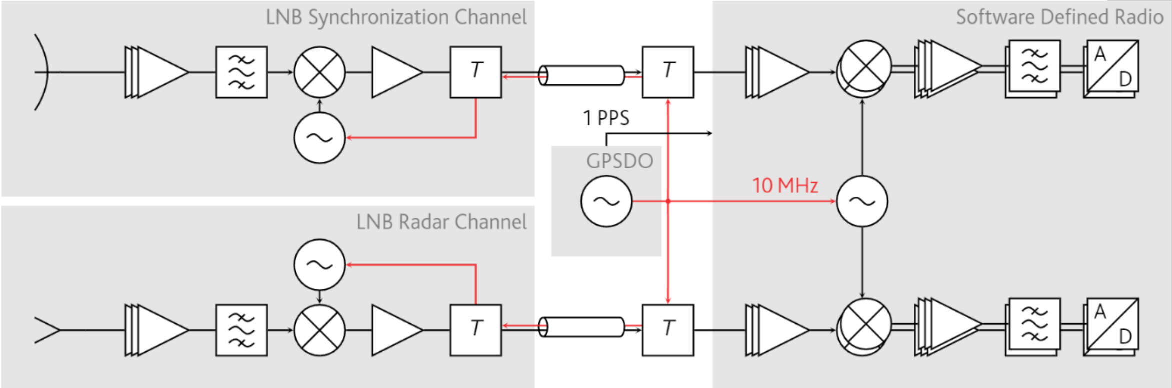

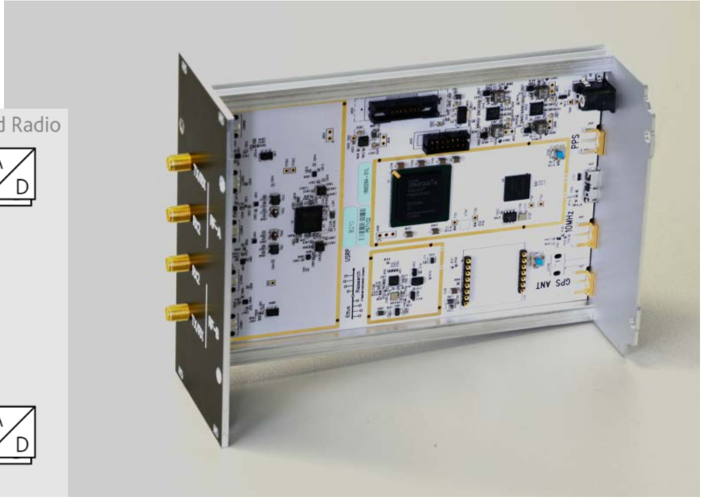


Google earth
N
1 km

Illuminator Intelsat 12

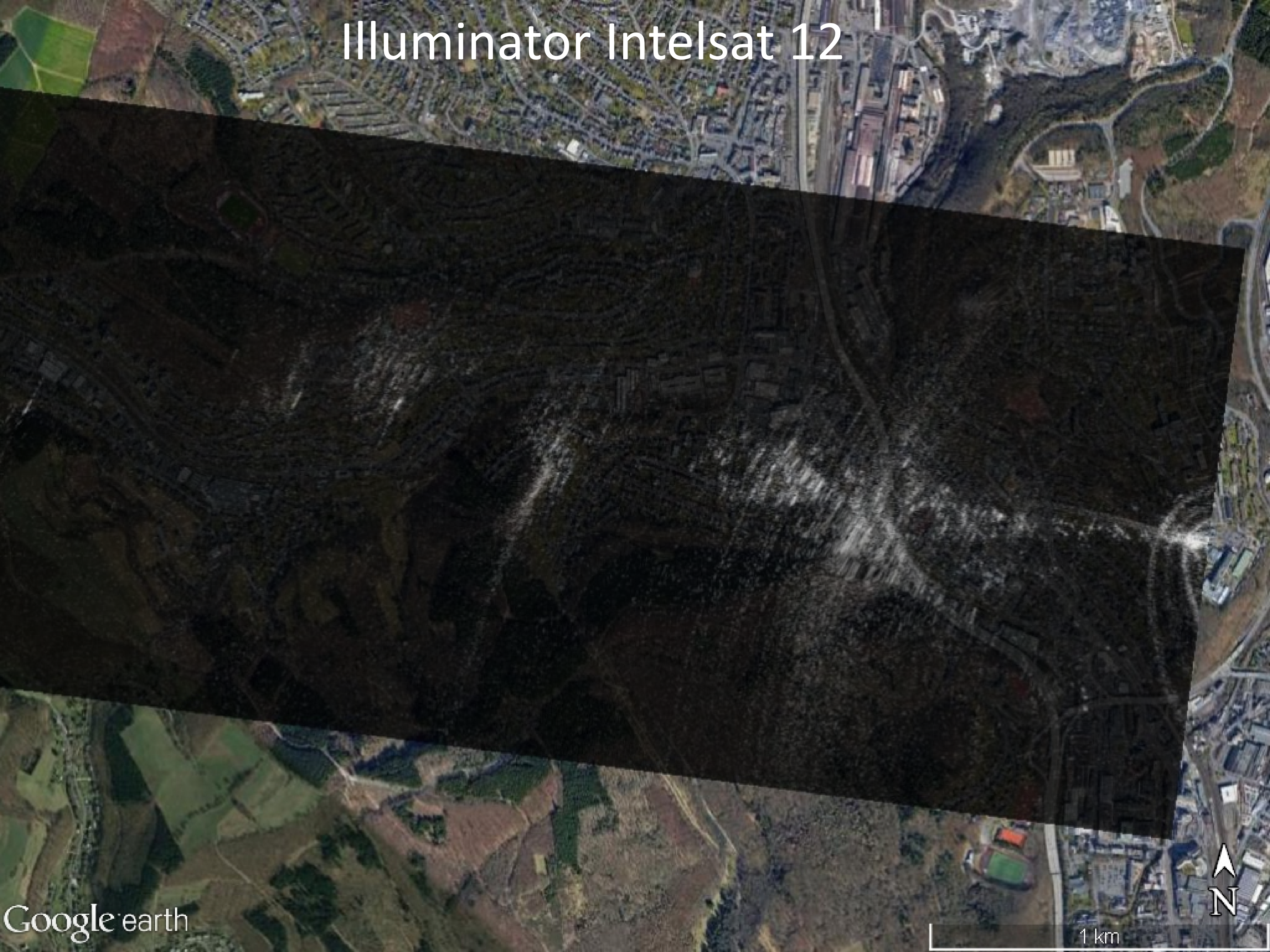

The (preliminary) end, but…

ZESS

CoSeRa 2018

5th International Workshop on Compressed Sensing applied to Radar, Multimodal Sensing and Imaging

10.–13. September 2018 – University of Siegen

UNIVERSITÄT SIEGEN

www.zess.uni-siegen.de/cosera2018

Thank you for your attention!